Abstract. The semiclassical limit of the focusing Nonlinear (cubic) Schrödinger Equation (NLS) corresponds to the singularly perturbed Zakharov Shabat (ZS) system that defines the direct and inverse scattering transforms (IST). In this paper, we derive explicit expressions for the leading order terms of these transforms, which are called semiclassical limits of the direct and inverse scattering transforms. Thus, we establish an explicit connection between the decaying initial data of the form $q(x,0) = A(x)e^{iS(x)}$ and the leading order term of its scattering data. This connection is expressed in terms of an integral transform that can be viewed as a complexified version of an Abel type transform. Our technique is not based on the WKB analysys of the ZS system, but on the inversion of the modulation equations that solve the inverse scattering problem in the leading order. The results are illustrated by a number of examples.

Semiclassical limit of the scattering transform for the focusing Nonlinear Schrödinger Equation

Alexander Tovbis* and Stephanos Venakides†

March 17, 2009

1 Introduction

Direct and inverse scattering transforms play the key role in the solution of integrable systems. Important results about the scattering transform with decaying initial data (potential) can be found in [26]. Our main interest lies in the semiclassical limit of the scattering transform for Zakharov - Shabat (ZS) system

$$i\varepsilon\frac{d}{dx}W=\begin{pmatrix} z & q \\ \bar{q} & -z \end{pmatrix}W\ , \tag{1}$$

where z is a spectral parameter, ε is a small positive parameter and W is a 2 by 2 matrix-function. ZS system (1) is the first (spatial) equation of the Lax pair for the focusing Nonlinear Shrödinger equation (NLS)

$$i\varepsilon\partial_t q+\frac{1}{2}\varepsilon^2\partial_x^2 q+|q|^2q=0\ , \tag{2}$$

where $x\in\mathbb{R}$ and $t\geq 0$ are space-time variables.

The scattering data, corresponding to the initial data $q(x,0,\varepsilon)$ consists of the reflection coefficient $r_{init}(z,\varepsilon)$, as well as of the points of discrete spectrum, if any, together with their norming constants. Since the time evolution of the scattering data is simple and very well known ([25]), the evolution of a given potential can be obtained through the inverse scattering of the evolving scattering data. The inverse scattering problem for the NLS (2) at the point x,t can be cast as a matrix Riemann-Hilbert Problem (RHP) in the spectral z-plane, which is stated as: find a 2×2 matrix-valued function $m(z)=m(z;x,t,\varepsilon)$, which depends on the asymptotic parameter ε and the external parameters x,t, such that: i) $m(z)$ is analytic in $\mathbb{C}\backslash\Gamma$, where the contour $\Gamma=\mathbb{R}$ with the natural orientation; ii)

$$m_+=m_-\begin{pmatrix} 1+r\bar{r} & \bar{r} \\ r & 1 \end{pmatrix}=m_-V \tag{3}$$

*Department of Mathematics, University of Central Florida, Orlando, FL 32816, email: atovbis@pegasus.cc.ucf.edu Supported by NSF grant DMS 0508779

†Department of Mathematics, Duke University, Durham, NC 27708, e-mail: ven@math.duke.edu Supported by NSF grant DMS 0707488

on the contour Γ, where $r(z,\varepsilon) = r_{init}(z,\varepsilon)\exp[\frac{2i}{\varepsilon}(2z^2t + zx)]$ and $m_\pm(z) = \lim_{\delta\to 0} m(z \pm i\delta)$ with $\delta > 0$ and $z \in \mathbb{R}$; iii) $\lim_{z\to\infty} m(z) = I$, where I denotes the identity matrix. In the presence of solitons the contour Γ contains additional small circles around the eigenvalues with the corresponding jump-matrices (see, for example, [22] or [13]).

In a more general setting, corresponding to AKNS systems, $\bar{r}(z)$ in the the jump matrix V should be replaced by $\rho(z)$, which represents another piece of the scattering data that is independent of $r(z)$; i.e., there is no functional dependence between $r(z)$ and $r^*(z)$ on $\mathbb{R}$; however, this case will not be considered in the present paper. It is well-known (see, for example [27]) that the RHP (3) has a unique solution $m(z)$ that has asymptotics $m(z) = I + \frac{m_1}{z} + O(z^{-2})$ as $z \to \infty$, and that the solution to the NLS (2) is given by $q(x,t,\varepsilon) = -2(m_1)_{12}$, where $(m_1)_{12}$ denotes the $(1,2)$ entry of matrix m_1. In the case when $r_{init}(z,\varepsilon)$ has analytic continuation into the upper halfplane, the RHP for $m(z)$ can be simplified by factorizing the jump matrix

$$V = \begin{pmatrix} 1 + rr^* & r^* \\ r & 1 \end{pmatrix} = \begin{pmatrix} 1 & \bar{r} \\ 0 & 1 \end{pmatrix} \begin{pmatrix} 1 & 0 \\ r & 1 \end{pmatrix} = V_- V_+ \quad , \tag{4}$$

and "splitting" jump condition (3) into two jumps: one with triangular jump matrix V_+ along some contour Γ_+ in the upper halfplane $\bar{\mathbb{C}}^+$ ($\mathbb{R}$ is included in $\bar{\mathbb{C}}^+$) and the other with triangular jump matrix V_- along some contour Γ_- in the lower halfplane $\bar{\mathbb{C}}^-$. Contours $\Gamma_\pm$ are deformations of $\mathbb{R}$. Due to the Schwarz symmetry of ZS problem, contours $\Gamma_\pm$ can be choosen to be symmetrical to each other with respect to the real axis, and we can restrict our attention to only one jump condition, say, on the contour $\Gamma_+ \subset \bar{\mathbb{C}}^+$.

A contour $\Gamma_+ \in \bar{\mathbb{C}}^+$, which is a smooth deformation of $\mathbb{R}$, together with a function $\tilde{f}(z)$, which is analytic (or even Hölder continuous) along Γ_+ with $\Im\tilde{f}(z) < -\delta$ for all suffisiently large $z \in \Gamma_+$, $\delta > 0$, define a solution $\tilde{q}(x,t,\varepsilon)$ of the NLS (2) in the following way: if $\tilde{m}(z)$ is the normed at $z = \infty$ solution of the matrix RHP with the jump matrix

$$V_+ = \begin{pmatrix} 1 & 0 \\ \tilde{r} & 1 \end{pmatrix}, \qquad \text{where} \qquad \tilde{r} = e^{-\frac{2i}{\varepsilon}\tilde{f}(z)} \tag{5}$$

on the contour Γ_+, and the corresponding symmetrical jump $V_- = V_+^*$ (see (4)) on the symmetrical contour Γ_-, than

$$\tilde{q}(x,t,\varepsilon) = -2(\tilde{m}_1)_{12}, \qquad \text{where} \qquad \tilde{m}(z) = I + \frac{\tilde{m}_1}{z} + O(z^{-2}) \tag{6}$$

as $z \to \infty$. This construction holds even if $\tilde{f}(z)$ depends on ε.

In the semiclassical limit problem (2), we consider initial data (potential) of the form

$$q(x,0,\varepsilon) = A(x)e^{iS(x)/\varepsilon}, \tag{7}$$

where the amplitude $A(x)$ is decaying at $\pm\infty$, and derivative of the phase $S'(x)$ has the limiting behavior

$$\lim_{x\to\pm\infty} S'(x) = \mu_\pm \tag{8}$$

with some finite μ_-, μ_+, $m_- \le \mu_+$. In order to calculate the leading order of the solution $q(x,t,\varepsilon)$, $t \ge 0$, one needs to find the leading order of the solution m to the RHP (3) as $\varepsilon \to 0$.

The nonlinear steepest descent method ([9], [10]), together with the g-function mechanism ([8]), is, perhaps, the most powerful tool of the asymptotic analysis of the RHP (3). The key part of this method, in the setting of our problem (genus zero region), is the following scalar RHP for the unknown function $g(z) = g(z; x, t)$, that: i) is analytic (in z) in $\bar{\mathbb{C}} \setminus \gamma_m$ (including analyticity at ∞); ii) satisfies the jump condition

$$g_+ + g_- = f_0 - xz - 2tz^2 \quad \text{on} \ \ \gamma_m, \tag{9}$$

for $x \in \mathbb{R}$ and $t \geq 0$, and; iii) has the endpoint behavior

$$g(z) = O(z-\alpha)^{\frac{3}{2}} \ + \ \text{analytic function in a vicinity of } \alpha. \tag{10}$$

Here: γ_m is a Schwarz-sym This observation remains true ifmetrical contour (called the main arc) with the endpoints $\bar{\alpha}, \alpha$, oriented from $\bar{\alpha}$ to α and intersecting $\mathbb{R}$ only at μ_+; $g_\pm$ are the values of g on the positive (left) and negative (right) sides of γ_m, and; function $f_0 = f_0(z)$, representing the scattering data, is Schwarz-symmetrical and Hölder-continuous on γ_m. Taking into the account Schwarz symmetry, it is clear that behavior of $g(z)$ at both endpoints α and $\bar{\alpha}$ should be the same. Assuming f_0 and γ_m are known, solution g to the RHP (9) without the endpoint condition (10) can be obtained by Plemelj formula

$$g(z) = \frac{R(z)}{2\pi i} \int_{\gamma_m} \frac{f(\zeta)}{(\zeta - z) R(\zeta)_+} d\zeta \ , \tag{11}$$

where

$$f(z) = f(z; x, t) = f_0(z) - xz - 2tz^2 \tag{12}$$

and $R(z) = \sqrt{(z-\alpha)(z-\bar{\alpha})}$. The branchcut of R coinsides with γ_m and the branch of R we use is defined by

$$\lim_{z \to \infty} \frac{R(z)}{z} = -1 \ . \tag{13}$$

If $f_0(z)$ is analytic in some region $\mathcal{S}$ that contains $\gamma_m \setminus \{\mu_+\}$, the formula for $g(z)$ can be rewritten as

$$g(z) = \frac{R(z)}{4\pi i} \int_{\hat{\gamma}_m} \frac{f(\zeta)}{(\zeta - z) R(\zeta)_+} d\zeta \ , \tag{14}$$

where $\hat{\gamma}_m \subset \mathcal{S}$ is a negatively oriented loop around γ_m (which is "pinched" to γ_m in μ_+, where f is not analytic) that does not contain z.

It is well known (see, for example, [12]) that additional smoothness at the endpoints put some constrains on the location of these endpoints. To state these constrains, we introduce function $h = 2g - f$. According to (14),

$$h(z) = \frac{R(z)}{2\pi i} \int_{\hat{\gamma}_m} \frac{f(\zeta)}{(\zeta - z) R(\zeta)_+} d\zeta \ , \tag{15}$$

where z is inside the loop $\hat{\gamma}_m$. The endpoint condition (10) can now be written as

$$h(z) = O(z-\alpha)^{\frac{3}{2}} \ \ \text{as} \ \ z \to \alpha, \tag{16}$$

or, equivalently,

$$\int_{\hat{\gamma}_m} \frac{f(\zeta)}{(\zeta-\alpha)R(\zeta)_+}d\zeta = 0 \ , \tag{17}$$

the latter equation known as a *modulation equation*. Substituting (12) into (17) yields

$$x + 2(\Re\alpha + \alpha)t = \frac{1}{2\pi i}\int_{\hat{\gamma}_m} \frac{f_0(\zeta)}{(\zeta-\alpha)R(\zeta)_+}d\zeta \ . \tag{18}$$

It is clear that for a given $f_0(z)$, (18) defines α as a function $\alpha = \alpha(x,t)$. The significance of $\alpha(x,t)$ is that it represents the leading ε-order term

$$q_0(x,t,\varepsilon) = A(x,t)e^{\frac{i}{\varepsilon}S(x,t)} \tag{19}$$

of the solution $q(x,t,\varepsilon)$ to the Cauchy problem (2)-(7) through

$$\alpha(x,t) = a(x,t) + ib(x,t) = -\frac{1}{2}S_x(x,t) + iA(x,t) \ . \tag{20}$$

By Schwarz symmetry, modulation equation (17) holds if α is replaced by $\bar{\alpha}$. Adding and subtracting these two equations and using integration by parts, we obtain system of *moment conditions*

$$\int_{\hat{\gamma}_m} \frac{f'(\zeta)}{R(\zeta)_+}d\zeta = 0 \ , \qquad \int_{\hat{\gamma}_m} \frac{(\zeta-a)f'(\zeta)}{R(\zeta)_+}d\zeta = 0 \ , \tag{21}$$

where $\alpha = a + ib$, which is equivalent to (17). If f_0 is defined only on the contour γ_m (nonanalytic case), the loop integrals in (21) should be replaced by the integrals over the contour γ_m. Substituting (12) into (21), we obtain

$$\frac{1}{2\pi i}\int_{\hat{\gamma}_m} \frac{f_0'(\zeta)}{R(\zeta)_+}d\zeta = x + 4ta \ , \qquad \frac{1}{2\pi i}\int_{\hat{\gamma}_m} \frac{(\zeta-a)f_0'(\zeta)}{R(\zeta)_+}d\zeta = -2tb^2 \ . \tag{22}$$

For a fixed $t \geq 0$, the second moment equation (22) defines a curve Σ in the spectral plane, whereas the first moment equation (22) determines a parametrization of Σ by $x \in \mathbb{R}$.

Solving system (22) for a given $f_0(z)$, i.e., finding $\alpha(x,t)$ that satisfies (22) for all $x \in \mathbb{R}$ and all $t \in [0,t_0]$ with some $t_0 > 0$, is the central part of the inverse scattering procedure for the leading order solution of the Cauchy problem (2)-(7). Considerable progress has been achieved in solving this problem, see [22], [13], [24]. However, calculating f_0, which represents the leading order term of the spectral data corresponding to (7), continue to pose a considerable challenge. In particular, the spectral data considered in [22] and [13] was calculated explicitly, because ZS system (1) for the corresponding initial data was reduced to the hypergeometric equation. In the case of general analytic initial data (7), the WKB analysis of singularly perturbed ZS systems (1) in the complex x-plane seems to be the most natural approach for the direct scattering. There are, however, considerable difficulties associated with this approach even for relatively simple initial data, such as, for example, the need to keep track of a large number of turning points, singularities, Stokes lines that connect them, etc., (see, for examle, [16]). This is why, in our opinion, the results about the direct scattering are quite limited: one can mention numerical simulations of the discrete spectrum

of (1) in [2], followed by formal WKB calculation in [16] of the Y-shaped spectral curve from [2], and rigorous WKB construction of discrete spectrum for certain special potentials (7) in [18].

The main goal of the present paper is to derive an explicit formula for $f_0(z)$ that will be valid for a rather broad class of initial data (7) directly from the moment conditions (21) (Section 2). We proceed with studying properties of the transforms that connect $f_0(z)$ with the scattering data (Sections 3 - 6) and, at the end, consider a number of examples that include already studied potentials (7), as well as some new cases (Section 7).

For the rest of the paper, unless specified otherwise, we assume $t = 0$. Then the first equation of (22) can be considered as a transformation

$$x(\alpha) = \frac{1}{\pi i}\int_{\gamma_m} \frac{f_0'(\zeta)}{\sqrt{(\zeta-\alpha)(\zeta-\bar\alpha)}_+}d\zeta \tag{23}$$

of a given $f_0'(\zeta)$ into $x(\alpha)$, which has the meaning of the inverse function to $\alpha(x) = \alpha(x,0), \quad x \in \mathbb{R}$. Provided that $\alpha(x)$, determined by initial data (7) through (20), is invertible for all $x \in \mathbb{R}$, $x(\alpha)$ is a real valued function defined on the curve Σ that is the graph of $\alpha(x), \quad x \in \mathbb{R}$. The main result of this paper is the formula

$$f_0(z) = \int_z^{\mu_+} \left[z - \mu_+ + \sqrt{(z-u)(z-\bar u)}\right] x'(u)du + (z-\mu_+)x(z) + f_0(\mu_+), \tag{24}$$

where $z \in \Sigma$ and the integral is taken along Σ, which is *the inversion* of transformation (23). Here $f_0(\mu_+)$ is a free real parameter and the branch of the radical satisfies normalization (13). Transformations (23) and (24) resemble the pair of *Abel transformants* for axially symmetric functions, which is convenient to write in the form ([1])

$$M(\xi) = -2\int_\xi^\infty N'(\eta)\sqrt{\eta^2-\xi^2}d\eta \qquad \text{and} \qquad N(\eta) = -\frac{1}{\pi}\int_\eta^\infty M'(\xi)\frac{d\xi}{\sqrt{\xi^2-\eta^2}}\,, \tag{25}$$

where $\xi, \eta \in \mathbb{R}$. Indeed, if $\alpha \in i\mathbb{R}$ and $\Sigma \subset i\mathbb{R}$, the radicals in (23) and (24) become $\sqrt{\zeta^2-\alpha^2}$ and $\sqrt{z^2-u^2}$ respectively, and transforms (23) and (24) become a pair of Abel transforms (with some extra terms in (24) required for convergence). However, if $\alpha \in \mathbb{R}$ and $\Sigma \subset \mathbb{R}$, (23) becomes finite Hilbert transform (note that, due to Schwarz symmetry, $f_0'(\zeta)$ has a jump $2i\Im f_0'(\zeta)$ along the real axis) on $[a, \mu_+]$. Transformations (23) and (24) will be referred to as *Abel-Hilbert (AH) or complexified Abel transformations* defined on a contour $\Sigma \subset \mathbb{C}$.

A given initial data (7) determines $\alpha(x) = \alpha(x,0)$ by (20), where $A(x,0) = A(x)$ and $S_x(x,0) = S'(x)$. We consider the following three objects, defined by initial data (7): 1) solution $q(x,t,\varepsilon)$ of the Cauchy problem (2), (7); 2) solution $\tilde q(x,t,\varepsilon)$ to (2) defined through (5)-(6), where $\tilde f = f_0(z) - xz - 2tz^2$ with $f_0(z)$ being the AH transformation of $x(\alpha)$ given by (24), and $\Gamma_+ = \Sigma$ (here we assume that $\alpha(x)$, $x \in \mathbb{R}$, is invertible with the inverse $x(\alpha)$; 3) function $q_0(x,t,\varepsilon)$ that is defined by (19), (20), where $\alpha(x,t)$ is a smooth in $x \in \mathbb{R}$ and $t \geq 0$ solution of the moment conditions (22) (analyticity of the initial data (7) on $x \in \mathbb{R}$ is required to define $q_0(x,t,\varepsilon)$ with $t > 0$). Since $q(x,0,\varepsilon) = q_0(x,0,\varepsilon)$ (transformation (23) is inverse to (23)), we call $q_0(x,t,\varepsilon)$ a *leading order semiclassical solution* to Cauchy problem (2), (7), or simply a *semiclassical solution*. The main achievement of this paper is formal

construction of the semiclassial solution $q_0(x,t,\varepsilon)$ with some positive t for a given analytic initial data (7). Does the semiclassical solution $q_0(x,t,\varepsilon)$ indeed represent a leading order behavior of $q(x,t,\varepsilon)$ for $t>0$? Although we do not have the general answer to this question, the following facts and observations indicate that the answer should be affirmative at least for some substantial class of the analytic initial data (7).

Requirements guaranteeing that $q_0(x,t,\varepsilon)$ is $O(\varepsilon)$ close to $\tilde{q}(x,t,\varepsilon)$ on a compact subset D of the x,t plane that do not contain breaking points (see below), can be found in [22], [24]. The first requirement is that

$$w(z)=\mathrm{sign}(\mu_+-z)\Im f_0(z)<0 \quad \text{for} \quad z<\mu_- \qquad \text{and for} \qquad z>\mu_+; \tag{26}$$

more precisely, $w(z)$ is separated from zero if $z<\mu_-$ and if $z>\mu_+$ except for neighborhoods of $\mu_\pm$, where it has behavior $O(z-\mu_\pm)$ respectively. Let γ_c be a bounded smooth oriented contour in the upper halfplane, called complementary arc, that connects α and μ_- and does not intersect γ_m (except at the common endpoint α). The second requirement is that for any $(x,t)\in D$ there exist main and complementary arcs γ_m and γ_c, connecting $\alpha(x,t)$ with $\mu_\pm$ respectively, such that the signs of $\Im h(z)$, where h is defined by (15), satisfy inequlities (sign distributions)

$$\Im h(z)<0 \quad \text{on both sides of } \gamma_m \qquad \text{and} \qquad \Im h(z)>0 \quad \text{on at least one side of} \gamma_c. \tag{27}$$

As shown in Section 5, violation of smoothness of $q_0(x,t,\varepsilon)$ in the process of time evolution leads to the break of the anzatz (19) for the semiclassical solution. Since (26) is independent of x,t, the break at some point (x_b,t_b) means that at least one of the inequalities (27) is violated at some point(s) $z_b\in\gamma_m\cup\gamma_c$, $z_b\neq\alpha(x_b,t_b)$, or that condition (16) becomes

$$h(z)=o(z-\alpha)^{\frac{3}{2}} \quad \text{as} \quad z\to\alpha, \tag{28}$$

if $z_b=\alpha(x_b,t_b)$. If z_b is not a branchpoint of $f_0(z)$ (regular break), then the situation can be corrected by introducing additional main and complementary arcs in the RHP (9)-(10), see [22] for details. This corresponds to the change of genus from zero to a positive even number (the genus is even because of Schwarz symmetry) of some hyperelliptic Riemann surface $\mathcal{R}(x,t)$ that shadows the evolution of $\tilde{q}(x,t,\varepsilon)$, see Remark 1.1 below. Correspondingly, the semiclassical solution $q_0(x,t,\varepsilon)$ can be expressed in terms of Riemann theta functions defined by $\mathcal{R}(x,t)$, and $O(\varepsilon)$ closeness between $q_0(x,t,\varepsilon)$ and $\tilde{q}(x,t,\varepsilon)$ extends to the region beyond the break. $O(\varepsilon)$ accurate approximation of $\tilde{q}(x,t,\varepsilon)$ by $q_0(x,t,\varepsilon)$ can be extended through further breaks (see [21]) provided that the breaks are regular. The case when z_b is a branchpoint of $f_0(z)$ (singular break) requires additional study. Approximation of $\tilde{q}(x,t,\varepsilon)$ by $q_0(x,t,\varepsilon)$ allows us to call $q_0(x,0,\varepsilon)$ the *semiclassical limit of the initial data* for solution $\tilde{q}(x,t,\varepsilon)$ (which is determined by $f_0(z)$).

Does q_0 approximate solution q of the Cauchy problem (2), (7)? The answer to this question depends on how accurately solution $\tilde{q}$ approximates solutions q. A closely related question is how accurately the scattering data $e^{-\frac{2i}{\varepsilon}\tilde{f}_0(z)}$ (see (5)) of $\tilde{q}$ approximates the scattering data $r_{init}(z,\varepsilon)$ of q. The authors are not aware of any general results of this nature, however, for a special family of initial data where explicit form of $r_{init}(z)$ is available (see [22]),

$$f_0(z)=\lim_{\varepsilon ra 0}\frac{1}{2}i\varepsilon\ln r_{init}(z,\varepsilon) \tag{29}$$

at every z in the domain of analyticity of $\ln r_{init}(z,\varepsilon)$ (with properly located branchcuts of $f_0(z)$). Similar result was obtained in [13] for pure soliton solutions of (2) ($r_{init} \equiv 0$), where $e^{-\frac{2i}{\varepsilon}\tilde{f}_0(z)}$ provided a good approximation to the corresponding discrete scattering data. The authors expect that (29) holds for a wide class of general analytic initial data. That is why $f_0(z)$, obtained by AH transformation (24), is called the *semiclassical limit of the scattering data* that corresponds to (7). The authors also expect that, subject to certain requirements, the semiclassical solution q_0 is the leading order approximation of q as $\varepsilon \to 0$. Establishing this fact seems to be the last remaining essential step towards the complete solution of the semiclassical asymptotic problem for the focusing NLS.

Remark 1.1. The RHP (9) can be modified to include N, $N \in \mathbb{N}$, contours (main arcs) where g undergoes a jump. These contours define a hyperelliptic Riemann surface $\mathcal{R} = \mathcal{R}(x,t)$ of the genus $N-1$, associated with the semiclassical limit of the initial value proble (Cauchy problem) (2)-(7). Higher genus of $\mathcal{R}$ indicates that the corresponding potential can be represented as a modulated N-phase wave expressed through the Riemann theta-functions, see, for example, [22]. The authors belive that the AH transformation (24) can be generalized to reperesent the semiclassical limit of the direct scattering transform for the higher genus cases, however, this paper is restricted to study potentials of the form (7) only, i.e., to genus zero potentials.

2 Inversion formula for the AH transform

In this section we prove that under the appropriate assumptions on $\alpha(x)$ the transformation (23) inverts the transformation (24). Let us assume that:

1. $\alpha(x) = -\frac{1}{2}S'(x) + iA(x)$ is a complex valued C^1 function on $\mathbb{R}$, where $A(x)$ is positive and $S'(x)$ satisfies (8);

2. $\alpha(x)$ is locally and globally invertible, i.e., $\alpha'(x) \neq 0$ on $\mathbb{R}$ and the graph S of $\alpha(x)$ does not have points of self-intersection;

3. the inverse function $x(\alpha)$, $\alpha \in \Sigma$, satisfies

$$\lim_{u \to \mu_+} (u-\mu_+)x(u) = 0, \quad u \in \Sigma, \qquad \text{and} \qquad (u-\mu_+)x'(u) \in L^1(\Sigma_{u_0}) \tag{30}$$

   for any $u_0 \in \Sigma$, where Σ_{u_0} denotes the arc of Σ connecting u_0 and μ_+.

Theorem 2.1. *If $\alpha(x)$ satisfies conditions 2 then $f_0(z)$ in* (24) *and its derivative are well defined. Moreover, transformation* (23) *is inverse to transformation* (24)*, i.e., the substitution of* (24) *into* (23) *turns the latter one into the identity.*

Proof. According to our choice (13) of the branch of the radical in (24), we have

$$\sqrt{(z-u)(z-\bar{u})} \sim -(z-\mu_+) \tag{31}$$

as $u \to \mu_+$ provided z is separeted from μ_+. Then

$$z - \mu_+ + \sqrt{(z-u)(z-\bar{u})} = -\frac{2(z-\mu_+)(\mu_+ - \Re u) + |\mu_+ - u|^2}{\left[z - \mu_+ - \sqrt{(z-u)(z-\bar{u})}\right]\sqrt{(z-u)(z-\bar{u})}}\,, \tag{32}$$

where, according to (31), the denominator approaches $-2(z-\mu_+)^2$ as $u \to \mu_+$. Now, convergence of the integral in (24) follows from (32) and the second condition of (30). Differentiation of (24) yields

$$f_0'(z) = \int_z^{\mu_+} \left[1 + \frac{z - \Re u}{\sqrt{(z-u)(z-\bar{u})}}\right] x'(u)du + x(z), \tag{33}$$

where the integrand can be expressed as

$$1 + \frac{z - \Re u}{\sqrt{(z-u)(z-\bar{u})}} = -\frac{(\Im u)^2}{\left[z - \mu_+ - \sqrt{(z-u)(z-\bar{u})}\right]\sqrt{(z-u)(z-\bar{u})}} \ . \tag{34}$$

Since $|\Im u| < |u - \mu_+|$, convergence of the integral in (33) follows from (34) and the second condition of (30).

Substituting of (33) into (23), which can be converted into

$$x(\alpha) = \frac{2}{\pi}\Im \int_{\mu_+}^{\alpha} \frac{f_0'(\zeta)}{\sqrt{(\zeta-\alpha)(\zeta-\bar{\alpha})}_+} d\zeta, \tag{35}$$

yields

$$\begin{aligned} x(\alpha) &= \frac{2}{\pi}\Im \int_{\mu_+}^{\alpha} \left[\int_{\zeta}^{\mu_+} \frac{1 + \frac{z-\Re u}{\sqrt{(z-u)(z-\bar{u})}}}{\sqrt{(\zeta-\alpha)(\zeta-\bar{\alpha})}} x'(u)du + \frac{x(\zeta)}{\sqrt{(\zeta-\alpha)(\zeta-\bar{\alpha})}}\right] d\zeta = \\ &= -\frac{2}{\pi}\Im \int_{\alpha}^{\mu_+} \left[x'(u)\int_{\alpha}^{u} \frac{1 + \frac{z-\Re u}{\sqrt{(z-u)(z-\bar{u})}}}{\sqrt{(\zeta-\alpha)(\zeta-\bar{\alpha})}} d\zeta + \frac{x(u)}{\sqrt{(u-\alpha)(u-\bar{\alpha})}}\right] du \end{aligned} \ . \tag{36}$$

Denote by

$$p(\zeta) = \frac{1 + \frac{z-\Re u}{\sqrt{(z-u)(z-\bar{u})}}}{\sqrt{(\zeta-\alpha)(\zeta-\bar{\alpha})}} \tag{37}$$

and by $\hat{\Sigma}$ a negatively oriented loop that contains contour $\Sigma_\alpha \cup \overline{\Sigma_\alpha}$. Then $\oint_{\hat{\Sigma}} p(\zeta)d\zeta = 0$ by Residue Theorem. If $\hat{\Sigma}_0$ denotes a negatively oriented loop around contour $\Sigma_u \cup \overline{\Sigma_u}$, and $\hat{\Sigma}_\pm$ denote positively oriented loops around contour $\Sigma_\alpha \setminus \Sigma_u$ and its complex conjugate respectively, see Figure 1, then

$$\oint_{\hat{\Sigma}_0} p(\zeta)d\zeta = \oint_{\hat{\Sigma}_+} p(\zeta)d\zeta + \oint_{\hat{\Sigma}_-} p(\zeta)d\zeta \ . \tag{38}$$

However, $\oint_{\hat{\Sigma}_0} p(\zeta)d\zeta = \oint_{\hat{\Sigma}_0} \frac{d\zeta}{\sqrt{(\zeta-\alpha)(\zeta-\bar{\alpha})}}$, since the remaining term of $p(\zeta)$ attains the same values on both sides of the branchcut $\Sigma_u \cup \overline{\Sigma_u}$. Taking into the account Schwarz symmetry of the intgrands, we obtain

$$\Im \int_{\alpha}^{u} p(\zeta)d\zeta = \Im \int_{\mu_+}^{u} \frac{d\zeta}{\sqrt{(\zeta-\alpha)(\zeta-\bar{\alpha})}} \ . \tag{39}$$

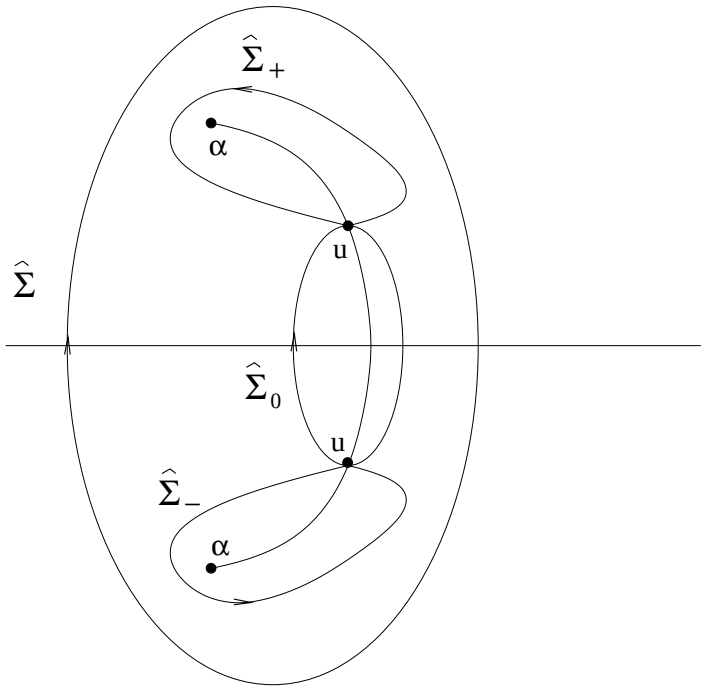

Figure 1: Contours $\hat{\Sigma}$, $\hat{\Sigma}_0$ and $\hat{\Sigma}_\pm$.

Returning to (36) and taking into the account (39) and the that $dx(u) = x'(u)du \in \mathbb{R}$ when $u \in \Sigma$, we obtain

$$\Im \int_\alpha^{\mu_+} \left[x'(u) \int_\alpha^u p(\zeta) d\zeta \right] du = \int_\alpha^{\mu_+} x'(u) \Im \left[\int_\alpha^u p(\zeta) d\zeta \right] du =$$
$$\int_\alpha^{\mu_+} x'(u) \Im \left[\int_{\mu_+}^u \frac{d\zeta}{\sqrt{(\zeta-\alpha)(\zeta-\bar{\alpha})}} \right] du = \Im \int_\alpha^{\mu_+} x'(u) \int_{\mu_+}^u \frac{d\zeta}{\sqrt{(\zeta-\alpha)(\zeta-\bar{\alpha})}} du \ . \quad (40)$$

Thus,

$$x(\alpha) = -\frac{2}{\pi} \Im \int_{\mu_+}^\alpha \left[x'(u) \int_{\mu_+}^u \frac{d\zeta}{\sqrt{(\zeta-\alpha)(\zeta-\bar{\alpha})}} + \frac{x(u)}{\sqrt{(u-\alpha)(u-\bar{\alpha})}} \right] du =$$
$$-\frac{2}{\pi}\, x(u) \Im \int_{\mu_+}^u \frac{d\zeta}{\sqrt{(\zeta-\alpha)(\zeta-\bar{\alpha})}} \Bigg|_{u=\alpha}^{u=\mu_+} = x(\alpha) \left(\frac{1}{2\pi i} \int_{\hat{S}} \frac{d\zeta}{\sqrt{(\zeta-\alpha)(\zeta-\bar{\alpha})}} \right) = x(\alpha) \ , (41)$$

where we used the fact that, according to the limit in (30), the contribution from $u = \mu_+$ is zero. □

3 Derivation of transformation (24) for $f_0(z)$

So far, the observation that transformation (23) resembles Abel transformation helped us to guess transformation (24), to which (23) is inverse. In this section, we will show how

transformation (24) can be derived from the analysis of the RHP (9). In particular, we show that solution $g(z)$ for the RHP (9), represented by integral (14) in the complex z-plane (Plemelj formula), can also be represented by a dual integral in the complex x-pane (see (62) below). The "input" data for the integral representation in the z-plane is $f_0(z)$ and x, whereas the "input" data for the dual integral representation in the x-plane is $\alpha(x)$ and z. Function $h(z)$ has similar integral representations. Then teh semiclassical limit of the spectral data $f_0(z)$ is given by $f_0 = 2g - h + xz$.

We start our derivation with the following observation.

Proposition 3.1. *Conditions* (9)-(10) *imply that* $\frac{\partial g(z)}{\partial \alpha} \equiv 0$.

Proof. Applying

$$\frac{\partial R(z)}{\partial \alpha} = -\frac{R(z)}{2(z-\alpha)} \tag{42}$$

and $\frac{1}{(\zeta-z)(\zeta-\alpha)} = \frac{1}{z-\alpha}\left[\frac{1}{\zeta-z} - \frac{1}{\zeta-\alpha}\right]$ to (11), we obtain

$$\frac{\partial g(z)}{\partial \alpha} = \frac{R(z)}{8\pi i(z-\alpha)} \int_{\hat{\gamma}_m} \frac{f(\zeta)}{(\zeta-\alpha)R(\zeta)_+} d\zeta. \tag{43}$$

But, according to (17), the integral in (43) is zero. The proof is completed. □

Under our convention $t = 0$, functions R, g, h, f depends on x and z. Since z will be considered as a parameter for the rest of the paper (unless specified otherwise), it is convenient for us henceforth to put the variable x in these functions in the first position. For example, the radical R introduced in (11) can be now rewritten as (44)

$$R(x,z) = \sqrt{(z-a(x))^2 + b^2(x)} \tag{44}$$

with the same choice of the branchcut in the z plane as before. The choice of the branchcut for $R(x,z)$ in the complex x-plane is discussed below.

Since $f(x,z) = f_0(z) - xz$, Proposition 3.1 implies that total derivatives

$$\frac{d}{dx}g(x,z) \equiv \frac{\partial}{\partial x}g(x,z), \qquad \text{and} \qquad \frac{d}{dx}h(x,z) \equiv \frac{\partial}{\partial x}h(x,z) \tag{45}$$

coincide with the corresponding partial derivatives. Differentiating both sides of the RHP (9) in x and using (10), we obtain

$$\frac{dh(x,z)}{dx} = -R(x,z), \qquad \frac{dg(x,z)}{dx} = -\frac{1}{2}[z + R(x,z)] \tag{46}$$

for all $x \in \mathbb{R}$ and $z \in \overline{\mathbb{C}^+}$, where z is considered as a parameter and $\mathbb{C}^\pm$ denotes the upper and the lower halfplane respectively (we also use notation $\mathcal{B}^\pm = \mathcal{B} \cap \mathbb{C}^\pm$ for any set $\mathcal{B}$). The fact that derivatives in (46) are independent of f opens the way to reconstruct $h(x,z)$, $g(x,z)$ and, thus, $f_0(z)$.

To construct $f_0(z)$, we require that

$$\alpha(x) = a(x) + ib(x) = -\frac{1}{2}S'(x) + iA(x) \tag{47}$$

satisfies the following conditions **(A)** :

1. $a(x)$ and $b(x)$ are real analytic on $\mathbb{R}$ and $b(x) > 0$;

2. all but finitely many points of the parametric curve

$$\partial\mathcal{E} = \{z \in \mathbb{C} : \ z = -S'(x)/2 \pm iA(x), \ x \in \mathbb{R}\} \tag{48}$$

are regular points, i.e., the tangent vector $\alpha'(x) \neq 0$, $x \in \mathbb{R}$; moreover, $\partial\mathcal{E}$ does not have points of self-intersection (note that we used notation Σ for $\partial\mathcal{E}^+$ in Sections 1, 2);

3. if $\mathcal{D}$ denotes the common domain of analyticity of $a(x), b(x)$, then $\alpha(\mathcal{D}) \supset \mathcal{L}$; here $\alpha(x)$ is defined by (47) and $\mathcal{L}$ is an open domain in the upper z-halfplane that contains the union of the strip $\{z : \ 0 \leq \Im z < L\}$, where $L > 0$, with $\overline{\mathcal{E}}^+$, where $\mathcal{E}$ denotes the open region of $\mathbb{C}$ bounded by $\partial\mathcal{E}$;

4. there exist $\mu_\pm \in \mathbb{R}$ and $p > 1$ such that

$$\lim_{\Re x \to \pm\infty} x^p \left[a(x) - \mu_\pm\right] = \lim_{\Re x \to \pm\infty} x^p b(x) = 0, \tag{49}$$

respectively for all x such that $\alpha(x) \in \mathcal{L}$;

The curve $\partial\mathcal{E}$ connects μ_+ and μ_- in both $\mathbb{C}^+$ and $\mathbb{C}^-$. Condition **A2** implies that there exists the inverse function $x(z)$, where $x(\alpha(x)) \equiv x \quad \forall x \in \mathbb{R}$. Note that $x(z)$ is analytic on $\partial\mathcal{E}^+$ at all the regular points. Any point $x^* \in \mathcal{D}$, such that $\alpha'(x^*) = 0$, is called a point of ramification. The corresponding z is called a logarithmic (log) point. We can analytically continue $x(z)$ from $\partial\mathcal{E}^+$ to $\mathcal{L}$ with the exception of the log points. To define $x(z)$ uniquely in, $\mathcal{L}$ we make branchcuts connecting every log point $z^* \in \mathcal{L}$, $\Im z > 0$ with $\mathbb{R} \cup \infty$ in such a way that they do not intersect $\mathcal{E}^+$ and keep $\mathcal{L}$ connected. Let $\mathcal{C}$ denote $\mathcal{L}$ with the cuts. Then $\mathcal{B} = x(\mathcal{C})$ is the image of $\mathcal{C}$ by the conformal map $x(z)$, see Fig. 2.

According to (46), we have

$$h(x, z) = -\int_{x(z)}^{x} R(y, z)dy \tag{50}$$

for all $z \in \mathcal{C}$ and all $x \in \mathcal{B}$, where the contour of integration lies in $\mathcal{B}$ and does not cross the branchcut $\Gamma(z)$ of $R(x, z)$ in the complex x-plane (z is fixed), which is a path connecting $x(z)$ with $-\infty$ (see Fig. 3).

For any fixed $z \in \mathcal{C}$, function $h(x, z)$ is analytic in x for all finite $x \in \mathcal{B}$ except the branchpoints $x = x(z)$ and $x = \overline{x(\bar{z})}$ of the radical R (the latter may or may not be in $\mathcal{B}$. On the other hand,

$$\frac{\partial h}{\partial z}(x, z) = -\int_{x(z)}^{x} \frac{z - a(y)}{\sqrt{(z - \alpha(y))(z - \tilde{\alpha}(y))}}dy + \frac{\sqrt{(z - \alpha(x(z)))(z - \tilde{\alpha}(x(z)))}}{\alpha'(x(z))} \ , \tag{51}$$

where

$$\tilde{\alpha}(x) = \overline{\alpha(\bar{x})} = a(x) - ib(x) \ . \tag{52}$$

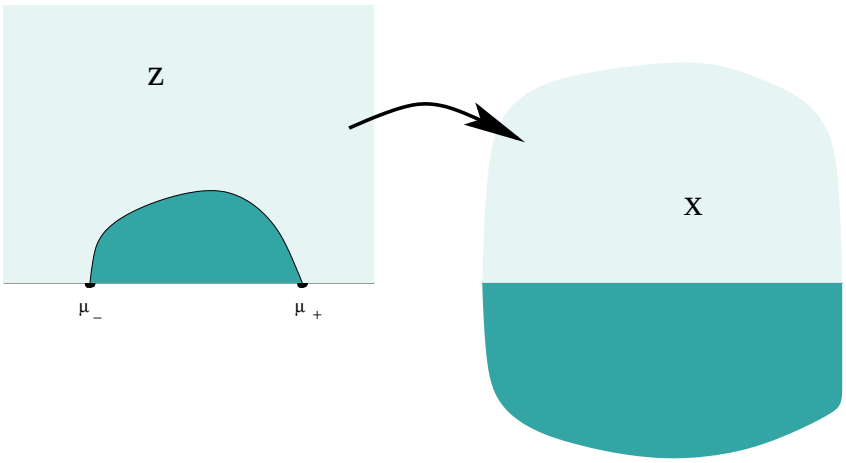

Figure 2: Map $x(z)$ maps $\partial\mathcal{E}^+$ into the real x-axis, $\overline{\mathcal{E}^+}$ (darker area) into $\mathcal{B}^-$ and the rest of $\mathcal{L}$ (lighter area) into $\mathcal{B}^+$. Possible cuts are not shown here.)

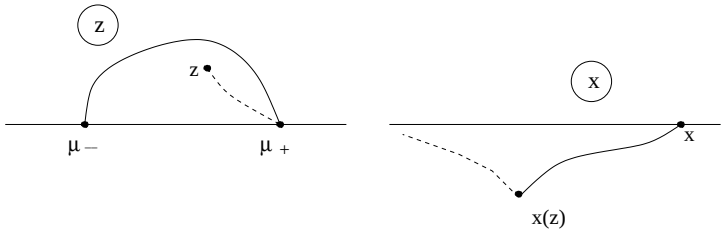

Figure 3: The branchcut of $R(x,z)$ is shown by the dashed lines: a path connecting $\alpha(x)$ and μ_+, x is fixed (left); a path connecting x and $-\infty$, z is fixed (right).

Since $\alpha(x(z)) \equiv z$ in $\mathcal{B}$, it is clear that the latter term is zero for all z except when $\alpha'(x(z)) = 0$, i.e., except when $z = \mu_\pm$ or z is a log point. So,

$$\frac{\partial h}{\partial z}(x,z) = -\int_{x(z)}^{x} \frac{z - a(y)}{\sqrt{(z-\alpha(y))(z-\tilde{\alpha}(y))}} dy \tag{53}$$

if $\alpha'(x(z)) \neq 0$. That means that for any finite $x \in \mathcal{B}$ function $h(x,z)$ is analytic in $z \in \mathcal{C}$ except for the log points, the branchpoints $z = \alpha(x)$, $z = \tilde{\alpha}(x)$, and, possibly, points $z = \mu_\pm$.

Does $h(x,z)$ from (50) coincide with h given by (15)? If the corresponding $\alpha(x)$ and $f_0(z)$ satisfy modulation equation (17), then they may differ by an independent of x constant. However, this constant is identically zero since $h(x(z),z) \equiv 0$ for all $z \in \mathcal{C}$ in both cases of (50) and (15). Thus, for any fixed $x \in \mathcal{B}$,

$$h(x,z) = O(z-\alpha(x))^{\frac{3}{2}} \quad \text{as} \quad z \to \alpha(x), \tag{54}$$

provided that $\alpha'(x) \neq 0$. Equation (54) also follows directly from (53). Finally, for all $x \in \mathbb{R}$, we extend $h(x,z)$ into the lower z-halfplane $\mathbb{C}^-$ by Schwarz reflection. Note that $h(x,z)$ has a jump $2i\Im h(x,z)$ for $z \in \mathbb{R}$. In the case $z \in \mathbb{C}^-$, the values of $h(x,z)$ can be analytically continued from $x \in \mathbb{R}$ to the complex x-plane.

To calculate $g(x,z)$, we first note that, according to (44), (13) and condition **A3**,

$$R(x,z) = -(z-\mu_\pm) + o\left(x^{-p}\right) \quad \text{as} \quad \Re x \to \pm\infty, \quad x \in \mathcal{D} \tag{55}$$

for any fixed $z \in \mathbb{C}$. Then

$$z - \mu_\pm + R(x,z) = \frac{2(z-\mu_\pm)[a(x)-\mu_\pm] - [a(x)-\mu_\pm]^2 - b^2(x)}{z - \mu_\pm - R(x,z)} = a(x) - \mu_\pm - \frac{R^2(x,\mu_\pm)}{2(z-\mu_\pm)} + o(x^{-2p}) \tag{56}$$

as $\Re x \to \pm\infty,\ x \in \mathcal{D}$, for any fixed $z \neq \mu_\pm$ respectively. According to (46), we define $g(x,z)$ as

$$g(x,z) = -\frac{1}{2}\left[\int_{+\infty}^{x} (z - \mu_+ + R(y,z))\, dy + \mu_+ x\right] + K(z) \tag{57}$$

for any finite $x \in \mathcal{B}$ and $z \in \mathcal{C}$, where $K(z)$ does not depend on x and the contour of integration is in $\mathcal{B}$. Convergence of the integral in (57) follows from (56).

Assuming that $\alpha(x)$ and $f_0(z)$ satisfy modulation equation (17), we want to determine $K(z)$ so that $g(x,z)$ defined by (57) coincide with $g(z)$ defined by (11). Note that

$$\lim_{x\to+\infty}\left[g(x,z) + \frac{1}{2}\mu_+ x\right] = K(z)\ . \tag{58}$$

Rewriting (11) as

$$g(x,z) = \frac{R(x,z)}{4\pi i}\int_{\hat{\gamma}_m} \frac{f_0(\zeta) - x\zeta}{(\zeta - z)R_+(x,\zeta)} d\zeta \tag{59}$$

and taking limit of (59) as $x \to +\infty,\ \ x \in \mathbb{R}$, $x \in \mathcal{B}$, we obtain, according to (55),

$$\lim_{x\to+\infty}\left[g(x,z) + \frac{1}{2}\mu_+ x\right] = \lim_{x\to+\infty}\left[\frac{(z-\mu_+)(f_0(\mu_+) - x\mu_+)}{4\pi i(z-\mu_+)}\int_{\hat{\gamma}_m} \frac{d\zeta}{\sqrt{(\zeta - \alpha(x))(\zeta - \overline{\alpha(x)})}} + \frac{1}{2}\mu_+ x\right] = \frac{1}{2}f_0(\mu_+). \tag{60}$$

Comaring (58) and (60), we obtain

$$K(z) = \frac{1}{2}f_0(\mu_+) \in \mathbb{R}, \tag{61}$$

the latter follows from the requirement that $g(x,z)$, $x \in \mathbb{R}$, is Schwarz-symmetrical in z. Thus, we obtain

$$g(x,z) = -\frac{1}{2}\left[\int_{+\infty}^{x} (z - \mu_+ + R(y,z))\, dy + \mu_+ x\right] + \frac{1}{2}f_0(\mu_+), \tag{62}$$

where $f_0(\mu_+)$ is a free real parameter.

We want to emphasize that (62) represents a new form of solution to the RHP (9)-(10) (with $t = 0$), written as an integral in the x-plane, see Theorem 3.2 below.

Note that for a finite fixed $z \in \bar{\mathbb{C}}^+$ function $g(x,z)$, defined by (62), is analytic for all finite $x \in \mathcal{B}$ except $x = x(z)$ and $x = \overline{x(\bar{z})}$. According to (55), we have

$$1 + \frac{z - a(x)}{R(x,z)} = \frac{a(x) - \mu_\pm}{z - \mu_\pm} + o(x^{-p}) \tag{63}$$

as $\Re x \to \pm\infty,\ x \in \mathcal{D}$, for any fixed $z \neq \mu_\pm$ respectively. Thus, for any finite $x \in \mathcal{B}$, function $g(x,z)$, defined by (62), is analytic in all finite $z \in \mathcal{C}$ except $z = \mu_+$ and branchpoints $z = \alpha(x),\ z = \tilde{\alpha}(x)$.

Now, using $f = 2g - h$, we obtain

$$f(x,z) = \int_{x(z)}^{+\infty} [z - \mu_+ + R(y,z)]\, dy + (z - \mu_+)x(z) - xz + f_0(\mu_+)\ , \tag{64}$$

so that

$$f_0(z) = \int_{x(z)}^{+\infty} [z - \mu_+ + R(y,z)]\, dy + (z - \mu_+)x(z) + f_0(\mu_+). \tag{65}$$

Since $h(x,z)$ and $g(x,z)$ are analytic in $z \in \mathcal{C}$ except the branchpoints $z = \alpha(x),\ z = \tilde{\alpha}(x)$, the log points and, possibly, points $z = \mu_\pm$, function $f_0(z) = 2g(x,z) - h(x,z) - xz$ is analytic over the same domain. But $f_0(z)$ does not depend on x, hence it is analytic everywhere in $\mathcal{C}$ except the log points and possibly, points $z = \mu_\pm$, with

$$f_0'(z) = \int_{x(z)}^{+\infty} \left[1 + \frac{z - a(y)}{R(y,z)}\right] dy + x(z). \tag{66}$$

Theorem 3.2. *For any $\alpha(x)$ satisfying conditions* **A1** - **A4**, *functions $g(x,z)$ and $f_0(z)$, given by* (62) *and* (65) *respectively, satisfy the RHP* (9)-(10) *all $x \in \mathbb{R}$ such that $\alpha'(x) \neq 0$.*

Proof. The contour γ_m in the RHP (9) can be deformed within the domain of analyticity of f_0 (endpoints $\alpha(x), \bar{\alpha}(x)$ and the midpoint μ_+ remain fixed) without affecting the solution $g(x,z)$. There are no more than a finitely many log points in any compact subset of $\bar{\mathcal{L}}$. According to the construction, set $\mathcal{C}$ is connected, i.e., without any loss of generality we can assume that γ_m lies within the domain of analyticity of f_0 (with the exception of the point μ_+). Let us fix some $x \in \mathbb{R}$, such that $\alpha'(x) \neq 0$, choose some z on the corresponding γ_m, and consider $g_+(z) + g_-(z)$. The contours of integration for $g_\pm$ in (62) lie on opposite sides of the branchcut of $R(x,z)$ in the complex x-plane (z is fixed), as shown on Fig. 4. Then

$$g_+(x,z) + g_-(x,z) = \int_{x(z)}^{+\infty} [z - \mu_+ + R(y,z)]\, dy + \int_x^{x(z)} (z - \mu_+) dy - \mu_+ x + f_0(\mu_+) = f(x,z)\ . \tag{67}$$

To prove that $g(x,z)$ is analytic at $z = \infty$ for any $x \in \mathcal{B} \setminus \{x(\infty)\}$, we fix some x and consider

$$\frac{\partial}{\partial z} g(x,z) = -\frac{1}{2} \int_{+\infty}^{x} \left(1 + \frac{z - a(y)}{R(y,z)}\right) dy\ , \tag{68}$$

where the contour of integration does not pass through $x(\infty)$. Then

$$R(y,z) = -(z - a(y)) + O\left(\frac{b^2(y)}{z - a(y)}\right) \tag{69}$$

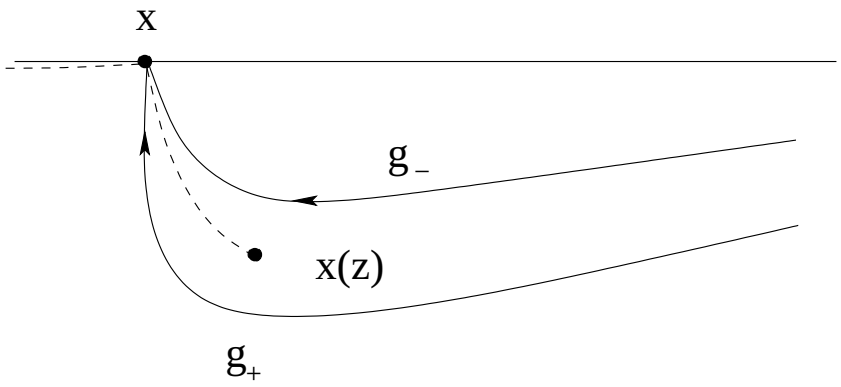

Figure 4: The branchcut of R in $\mathcal{B}$, connecting $x(z)$ and $-\infty$ is shown by the dashed line, contours of integration for $g_\pm$ are shown by solid lines.

as $z \to \infty$ uniformly on the contour of integration. Therefore, the integrand in (68) is of the order $O(b^2(y))$ uniformly on the contour of integration as $z \to \infty$, so that $\frac{\partial}{\partial z} g(x,z)|_{z=\infty}$ is well defined. Proof of (10) follows from (54) and the fact that $f_0(z)$ is analytic at $z = \alpha(x)$. Thus, requirements i) - iii) of the RHP (9)-(10) are satisfied. □

Remark 3.3. Theorem 3.2 remains true if in the expressions for $g(x,z)$ and $f_0(z)$ we replace $+\infty$ with $-\infty$ and μ_+ with μ_-.

Remark 3.4. For any $z \in \mathcal{E}^+$, the contour of integration in (64) is the interval $[x(z), \infty)$ of the real axis. Then the change of variables $u = \alpha(y)$ converts (64) into the transformation (24). Note that this is not true for $z \notin \mathcal{E}^+$, since $\bar{u} \neq \overline{\alpha(\bar{y})}$ for complex y.

4 Inequalities (27)-(26) for f_0

In Sections 2 and 3 we constructed the semiclassical limit of the scattering data $f_0(z)$ for ZS system (1) with a given potential (7). Let us assume that potential (7) satisfied conditions **A**. In this section we discuss inequalities (26) for f_0 as well as existence of the main and the complementary arcs satisfying (27) for all $x \in \mathbb{R}$.

We start with the observation that for any $x \in \mathbb{R}$ we have

$$\Im h(x, \mu_\pm) = -\Im \int_{\pm\infty}^{x} \sqrt{(\mu_\pm - \alpha(y))(\mu_\pm - \overline{\alpha(y)})}dy = 0 \ , \tag{70}$$

since the contour of integration lies on the real line and the integrand is real valued. Convergence of the integral in (70) follows from (49).

Let us consider $w(z), z \in \mathbb{R}$. According to (26), (50) and Schwarz symmetry of $g(x,z)$, $x \in \mathbb{R}$, we have

$$w(z) = \mathrm{sign}(\mu_+ - z)\Im \int_{x(z)}^{x} \sqrt{(z - \alpha(y))(z - \tilde{\alpha}(y))}dy, \tag{71}$$

where $x \in \mathbb{R}$ can be choosen arbitrarily, i.e., the right hand side of (71) does not depend on a particular choice of $x \in \mathbb{R}$. Therefore, we can choose contour of integration in (71) as the

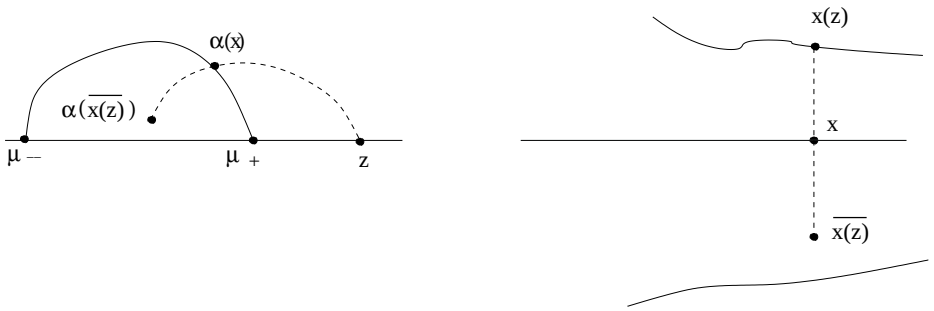

Figure 5: Two solid curves in the x-plane show the boundaries of $\mathcal{B}$. The image of the segment $[x(z), \overline{x(z)}]$ in z-plane is shown by the dashed line.

vertical segment $[x(z), x]$, where $x = \Re x(z)$, traversed in the negative direction, i.e., down (note that $\Im x(z) > 0$).

Lemma 4.1. *If*

$$|\arg(z - \alpha(y)) - \arg(z - \alpha(\bar{y}))| \leq \pi \tag{72}$$

for every $y \in [x(z), \Re x(z)]$*, where* $z > \mu_+$*, then* $w(z) < 0$*. If*

$$|\arg(z - \alpha(y)) - \arg(z - \alpha(\bar{y})) - 2\pi| \leq \pi \tag{73}$$

for every $y \in [x(z), \Re x(z)]$*, where* $z < \mu_-$*, then* $w(z) < 0$*.*

Proof. Consider, for example, the case $z > \mu_+$. Since dy is negative purely imaginary, it is sufficient to show that $\Re\sqrt{(z - \alpha(y))(z - \tilde{\alpha}(y))} < 0$. Taking into account our determination of the square root (13), the latter condition is equivalent to $|\arg(z-\alpha(y))+\arg(z-\tilde{\alpha}(y))| \leq \pi$, which, together with (52), implies (72), see Fig. 5. Similar arguments prove the remaining case $z < \mu_-$. □

Remark 4.2. Listed below are some sufficient conditions for (72) and (73) to be true for some $z > \mu_+$ or some $z < \mu_-$ respectively.

1. $w(z) < 0$ for some $z > \mu_+$ or some $z < \mu_-$ provided

$$[x(z), \overline{x(z)}] \subset \mathcal{B}. \tag{74}$$

Indeed, this condition implies that and $\alpha(\bar{y}) \in \mathcal{E}^+$ for any $y \in [x(z), x]$, see Fig. 5. Since $\alpha(y) \in \mathbb{C}^+ \setminus \mathcal{E}$, the inequality (72) is satisfied. Similar considerations are valid for (73). Condition (74) is satisfied if, for example, the upper boundary $\partial\mathcal{B}^+$ satisfies the vertical line test and if the complex conjugate $\overline{\partial\mathcal{B}^+} \subset \mathcal{B}$.

2. According to lemma 4.1, $w(z) < 0$ for some $z > \mu_+$ provided that for every $y \in [x, x(z)]$ the angle between $z - \alpha(y)$ and $z - \alpha(\bar{y})$ is less than π. This happens, for example, if one can draw a line l through the point z so that the curve $\alpha(y)$, $y \in [x(z), \overline{x(z)}]$ does not cross l (lies in one the halfplanes produced by l). In particular, if l is a vertical line, we obtain

$$\Re\alpha(y) \leq z \tag{75}$$

respectively for all $y \in [x(z), \overline{x(z)}]$. Similar results hold for $z < \mu_-$.

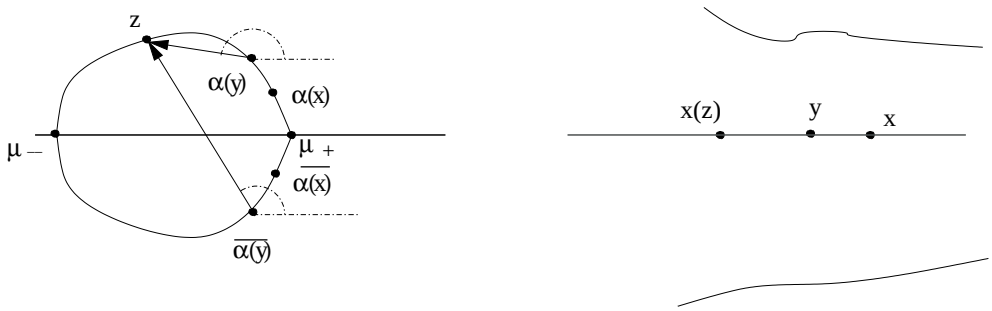

Figure 6: Vectors $z-\alpha(y)$ and $z-\overline{\alpha(y)}$ for $y\in[x(z),x]\subset\mathbb{R}$.

We now consider inequality (27) under additional assumption that $a(x)$ is a monotonically increasing function. We choose γ_c^+ to be the part of $\partial\mathcal{E}^+$ connecting $\alpha(x)$ and μ_-. Take any $z\in\gamma_c^+$. Then $x(z)$ is real and $x(z)<x$. Let us choose any $y\in[x(z),x]$, it is easy to check, (see Fig. 6) that

$$0\le\arg\Big((z-\alpha(y))(z-\overline{\alpha(y)})\Big)\le 2\pi\ , \tag{76}$$

so that, taking into account (50) and (13), we obtain $\Im h(x,z)>0$ on γ_c.

Let us now study the sign of $\Im h(x,z)$ on the main arc γ_m^+. Notice that $h_+ + h_- \equiv 0$ on γ_m, so that, in general, $\Im h$ has opposite signs on opposite sides of γ_m. Therefore, we have to have $\Im h\equiv 0$ on γ_m. Let us first find sign$\Im h$ on the arc of $\partial\mathcal{E}^+$ between $\alpha(x)$ and μ_+. Equivalently, we can think of deforming γ_m^+ to the above mentioned arc of $\partial\mathcal{E}^+$ and finding sign$\Im h$ on the negative (external) side of the arc. It is easy to see that if point z will pass over $\alpha(x)$ outside (of $\mathcal{E}$), then the sum of the angles, shown at Fig. 6, i.e., $\arg\Big((z-\alpha(y))(z-\overline{\alpha(y)})\Big)$, satisfies inequalities (76). Repeating the previous arguments, we readily obtain $\Im h(x,z)<0$, $z\in\partial\mathcal{E}^+$ between $\alpha(x)$ and μ_+ on the outer (negative) side of the contour. Of course, on the opposite (positive) side of the branchcut, $\Im h(x,z)>0$. That means, that inequalities on γ_m^+ will be satisfied if there exists a branch of the level curve $\Im h=0$ ($x\in\mathbb{R}$ is fixed), connecting μ_+ and $\alpha(x)$. This question is discussed below.

We now want to calculate $\frac{\partial h}{\partial z}(x,\mu_+^+)$ by taking limit $z\to\mu_+$ along the negative (outer) side of γ_m^+ (it is still asumed that γ_m deformed to coincide with arc of $\partial\mathcal{E}^+$ connecting $\alpha(x)$ and μ_+). According to (53),

$$\frac{\partial h}{\partial z}(x,z)=\int_x^{x(z)}\frac{z-a(y)}{\sqrt{(z-\alpha(y))(z-\overline{\alpha(y)})}}dy\ . \tag{77}$$

Therefore, the fact that

$$0<\varphi-\frac{1}{2}(\varphi_1+\varphi_2)<\pi\ , \tag{78}$$

where $\varphi=\arg(z-a(y))$, $\varphi_1=\arg(z-\alpha(y))$, $\varphi_2=\arg(z-\overline{\alpha(y)})$, together with the determination of the proper branch of the radical $R(y,z)$, imply $\Im\frac{\partial h}{\partial z}(x,z)<0$ in (77).

To prove (78), we first notice that the monotonicity of $a(x)$ on $\mathbb{R}$ implies

$$0<\varphi\le\frac{\pi}{2},\quad -\frac{\pi}{2}\le\varphi_1<\frac{\pi}{2},\ \ 0<\varphi_2\le\frac{\pi}{2},\ \ \varphi_2\ge\varphi\ge|\varphi_1|, \tag{79}$$

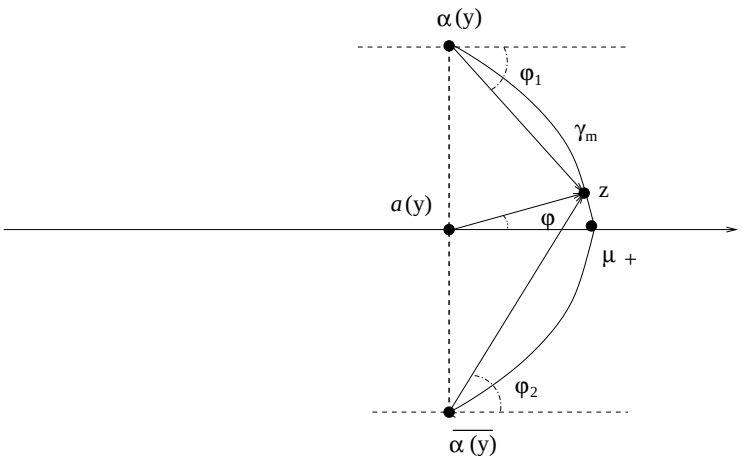

Figure 7: Angles φ_1 (negative), φ_2 and φ for $\alpha(y)$, where $x \le y \le x(z)$.

see Fig. 7, so that the second inequality of (78) follows from (79). Notice that $\beta_1 > \beta_2$, where $\beta_1 = \frac{\pi}{2} + \varphi_1$, $\beta_2 = \frac{\pi}{2} - \varphi_2$. Then the remaining inequality (78) becomes

$$2\varphi > \beta_1 - \beta_2 \ . \tag{80}$$

Let us inscribe the triangle $\alpha(y), z, \overline{\alpha(y)}$ into the circle. As shown on Fig. 8, cases $\varphi_1 < 0$ and $\varphi_1 > 0$, both angles $\beta_1 - \beta_2$ and 2φ rest on the arc $z, O, \bar{z}$. Then (80) follows from the fact that the vertex of angle $\beta_1 - \beta_2$ is on the circle, whereas the vertex of angle 2φ is inside the circle. Thus, (78) is proven.

The fact that $\lim_{z\to\mu_+^+} \Im\frac{\partial h}{\partial z}(x,z)$, if exists, is negative implies

$$w'(\mu_+^+) = -\lim_{z\to\mu_+^+} \Im\frac{\partial h}{\partial z}(x,z) > 0\text{`}. \tag{81}$$

Choosing the other branch of $R(y,z)$, we obtain

$$w'(\mu_+^-) = -\lim_{z\to\mu_+^-} \Im\frac{\partial h}{\partial z}(x,z) < 0 \tag{82}$$

if the limit exists, where μ_+^- is on the positive (inetrior) part of γ_m.

Equations (70), (81) and (82) show that $\Im h(x,z)$ is negative for real z in a vicinity of μ_+. Thus, there exists a zero level curve λ of $\Im h(x,z)$ emanating from $z = \mu_+$ into the upper half-plane. Suppose that $\lambda \subset \mathcal{C}$ and connects μ_+ with $\alpha(x)$. Then the signs of $\Im h$ to the right and to the left of λ have to be negative, i.e., the first inequality in (27) is satisfied. The results of this section can be summarized by the following statement.

Statement 4.3. *Let initial data* (7) *be such that: assumptions* **(A)** *are satisfied and* $S'(x)$ *is monotone on* $\mathbb{R}$*;* $w(z)$ *satisfies inequalities* (26)*. If for a given* $x \in \mathbb{R}$ *a zero level curve* λ*, emanating from* μ_+*, passes through* $\alpha(x)$ *and does not intersect branchcuts of* f_0*, then* $q_0(x,0,\varepsilon)$ *is* $O(\varepsilon)$ *approximation of* $\tilde{q}(x,0,\varepsilon)$*.*

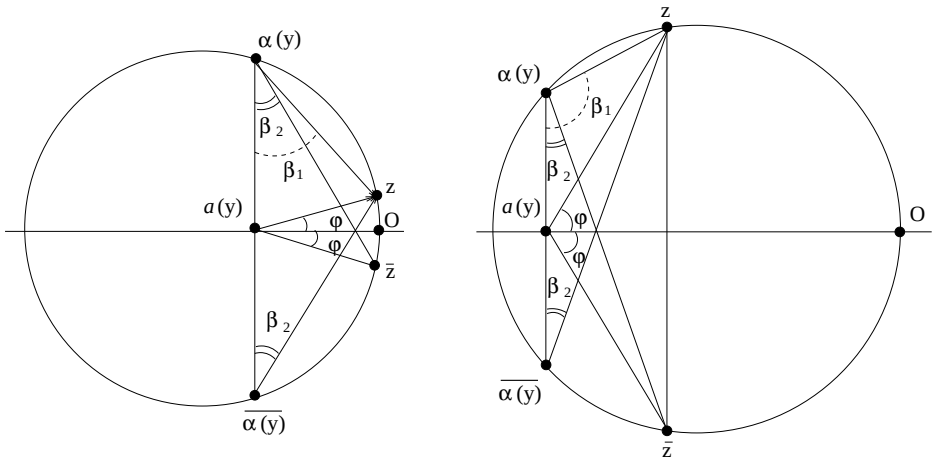

Figure 8: Triangle $\alpha(y), z, \overline{\alpha(y)}$ inscribed in a circle. The left circle shows the case $\varphi_1 < 0$, the right circle shows the case $\varphi_1 > 0$.

5 Some geometrical aspects of transition to a higher genus (breaking)

In this section we consider t assuming nonnegtive values. Functions f and h are defined by (12) and (15) respectively. As it was established in [22], [24], transition from the genus zero to a higher genus (genus 2) occurs when an additional branch of zero level curve of $\Im h(x,t,z)$ (the branch that begins and ends at $z=\infty$) intersects with the contour $\gamma^+ = \gamma_m^+ \cup \gamma_c^+$ at some point $z_b = z_b(x,t)$, which is not a log point (the case of g^+ intersecting a log point requires further investigation). There are at least four zero level curves of $\Im h(x,t,z)$ passing through the point $z = z_b(x,t)$, which implies that $h_z(x,t,z_b) = 0$. In the case $z_b(x,t) \neq \alpha(x,t)$, the point z_b is called a double point. There are exactly four zero level curves of $\Im h(x,t,z)$ passing through a double point z_b (degenerate cases of multiple level curves collision are not considered here, however, see [21]). In the remaining case $z_b(x,t) = \alpha(x,t)$, a triple point. There are five zero level curves of $\Im h(x,z,t)$ passing through a nondegenerate triple point $z_b(x,t)$. The breaking point x_b, t_b on the x,t plane that corresponds to a triple point z_b is the starting point of the breaking curve that separates the genus zero and genus two regions for $t \geq t_b$. Typically, the breaking curve forms a corner at x_b, t_b. A regular point of the breaking corve corresponds to a double point z_b. The simple modulated wave $q_0(x,t,\varepsilon)$ (semiclassical solution), given by (19), (20) fails to approximate solution $\tilde{q}(x,t,\varepsilon)$ in the genus two region beyond $t = t_b$. In this region $\tilde{q}$ can be approximated by a two-phase modulated wave constructed through Riemann theta functions (see [22]). The onset of a two-phase wave (genus two) behavior of $\tilde{q}$ corresponds to the appearance of a triple point $\alpha(x_b, t_b)$ on the spectral plane. The main result of this section is that at the first breaking point x_b, t_b the semiclassical solution $q_0(x,t,\varepsilon)$ loses its smoothness. More precisely, if $\alpha(x,t)$ is a triple point for some $x = x_b, t = t_b$ then the derivative $\alpha_x(x_b,t_b) = \infty$. In other words, genus zero anzatz $q_0(x,t,\varepsilon)$ experiences the first break at $t = t_b$ only if the amplitude of q_0 or derivative of its phase (or both) develops an infinite slope at $x = x_b$. The proof uses representation (50) of $h(x,z) = h(x,t_b,z)$, where t_b is fixed, as an integral in the complex x-plane.

Lemma 5.1. *If assumptions* **A** *for $\alpha(x) = \alpha(x, t_b)$ are satisfied then for any fixed $x \in \mathbb{R}$ we have*

$$\frac{\partial}{\partial z} h(x,z) = \frac{\sqrt{ib(x)}}{\sqrt{2}\alpha'(x)} \sqrt{z - \alpha(x)} + O(z - \alpha(x))^{3/2} \tag{83}$$

in a vicinity of the branchpoint $z = \alpha(x)$, provided $\alpha(x)$ is not a log point.

Proof. Since $\alpha(x)$ is not a log point, we have

$$x(\alpha(x) + \delta) = x + \frac{dx}{dz}\delta + o(\delta) = x + \frac{\delta}{\alpha'(x)} + o(\delta),$$

where $\delta \in \mathbb{C}$ is a small. Using (53), we calculate

$$\begin{aligned} \left.\frac{h_z(x,z)}{R(x,z)}\right|_{z=\alpha(x)} &= \lim_{\delta \to 0} \frac{1}{R(x, \alpha(x) + \delta)} \int_x^{x + \frac{\delta}{\alpha'(x)}} \frac{z - a(y)}{\sqrt{(z - \alpha(y))(z - \tilde{\alpha}(y))}} dy = \\ &\lim_{\delta \to 0} \frac{ib(x) + \delta}{\alpha'(x)(2ib(x) + \delta)} = \frac{1}{2\alpha'(x)} \ , \end{aligned} \tag{84}$$

which implies (83). □

As an immediate consequence of Lemma 5.1, we obtain

$$h(x,z) = \left[\frac{\sqrt{2ib(x)}}{3\alpha'(x)} + O(\sqrt{z - \alpha(x)}) \right] (z - \alpha(x))^{3/2} \ . \tag{85}$$

It is well known that zero genus anzatz for zero dispersion limit of the KdV equation breaks down when it develops infinite slope. The following corollary, which is another immediate consequence of Lemma 5.1, is an analog of this statement for the focusing NLS equation.

Corollary 5.2. *In the conditions of Lemma 5.1 $\alpha(x_b) = \alpha(x_b, t_b)$ is a triple point only if $\alpha'(x_b) = \infty$.*

Proof. $\alpha(x_b)$ is a triple point only if the leading term of (85) is zero. Since $b(x) > 0$ on $\mathbb{R}$ (condition **A1**), we conclude that $\alpha'(x_b) = \infty$. □

Remark 5.3. According to [5], solution $q(x, t, \varepsilon)$ to Cauchy problem (2), (7) develops *elliptic umbilic singularity* at (x_b, t_b) if $\alpha(x_b, t_b)$ is a triple point. It is hypotesized there that in a vicinity of (x_b, t_b) a solution $q(x, t, \varepsilon)$ can be approximated by the special *tritronqee* solution of the first Painleve equation P1 (see [5] for further details).

An obvious geometrical interpretation of Corollary (5.2) is the curve $\alpha(x)$ in $\mathbb{R} \times \mathbb{C}$, where $x \in \mathbb{R}$ and $\alpha(x) \in \mathbb{C}$. For any $x \in \mathbb{R}$, this curve has a unique intersection with the plane perpendicular to $\mathbb{R}$ at x, which we interpret as a spectral plane $\mathbb{C}$, see Fig. 9. This property is preserved under the NLS evolution $\alpha(x,t) = a(x,t) + ib(x,t)$, where $\alpha(x,0) = \alpha(x)$, as long as (x,t) is in the genus zero region. To get to a higher genus region, the curve $\alpha(x,t)$ must develop a "fold" (at least in the solitonless case), shown at Fig. 10. It is clear from the topological point of view that $\alpha(x,t)$ should become tangential to the spectral plane at some (x_b, t_b) before the fold can develop, see Fig. 11. The point (x_b, t_b) correspond to a triple point. Geometricaly, it is clear that $\alpha_x(x_0, t_0) = \infty$, which is exactly the statement of Corollary (5.2).

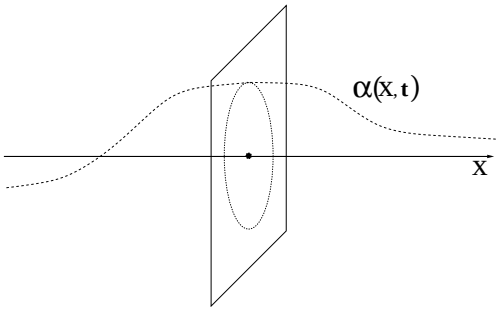

Figure 9: Curve $\alpha(x,t)$ in $\mathbb{R}\times\mathbb{C}$, spectral plane $\mathbb{C}$ is orthogonal to real x-axis. Genus zero case.

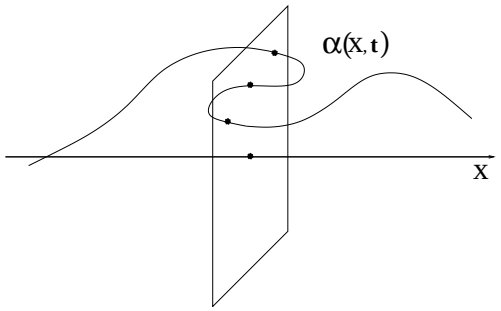

Figure 10: Curve $\alpha(x,t)$ in $\mathbb{R}\times\mathbb{C}$, spectral plane $\mathbb{C}$ is orthogonal to real x-axis. The curve developed a "fold". Three point of intersection of $\alpha(x,t)$ and the spectral plane are indicated. For the values of x, corresponding to the "fold", points (x,t) belong to the genus two region.

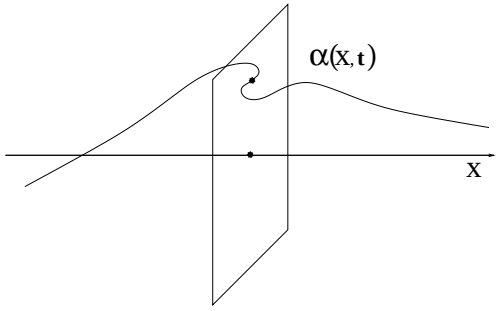

Figure 11: Curve $\alpha(x,t)$ in $\mathbb{R}\times\mathbb{C}$, spectral plane $\mathbb{C}$ is orthogonal to real x-axis. The point of tangency between $\alpha(x,t)$ and $\mathbb{C}$ corresponds to a triple point.

6 Symmetry

In this section we establish connections between the symmetry of the initial and the scattering data.

Statement 6.1. *Initial data $q(x,0) = q(x,0,\varepsilon)$ given by (7) is even iff*

$$\alpha(-\bar{x}) = -\overline{\alpha(x)} \ . \tag{86}$$

for all x in the domain of analyticity $\mathcal{D}$ of $\alpha(x)$. Here $\alpha(x) = a(x)+ib(x) = -\frac{1}{2}S'(x)+iA(x)$.

Proof. If $q(x,0)$ is even then $a(x)$ is odd and $b(x)$ is even. Then $\alpha(-\bar{x}) = -a(\bar{x}) + ib(\bar{x}) = -[\overline{a(x)} - i\overline{b(x)}] = -\overline{\alpha(x)}$. Conversly, taking $x \in \mathbb{R}$, we obtain $a(-x) + ib(-x) = \alpha(-\bar{x}) = -\overline{\alpha(x)} = -a(x) + ib(x)$. □

Statement 6.2. *Equation (86) is equivalent to*

$$x(-\bar{z}) = -\overline{x(z)} \tag{87}$$

that holds for all $x \in \mathcal{B}$.

Proof. $x = x(z) \ \Leftrightarrow \ z = \alpha(x) \Leftrightarrow \ -\bar{z} = -\overline{\alpha(x)}$. Then, according to (86), $-\bar{z} = \alpha(-\bar{x})$, so that $x(-\bar{z}) = -\overline{x(z)}$. Proof of the converse statement is similar. □

Before proving the next statement, it's worth reminding that the radical $R(x,z)$ with a fixed x has a branchcut $\gamma(x) = \gamma_m$ connecting $\alpha(x)$ and $\tilde{\alpha}(x) = \overline{\alpha(\bar{x})}$ that passes through μ_+.

Statement 6.3. *If $\alpha(x)$ is an odd function or if $\alpha(x)$ satisfies (86) then*

$$R^2(-\bar{x},-\bar{z}) = \overline{R^2(x,z)} \ , \tag{88}$$

for all $\Im z \geq 0$ and all $x \in \mathcal{D}$. The converse is also correct.

Proof. Equation (88) can be written as

$$[(z-\alpha(x))(z-\overline{\alpha(\bar{x})})] = \overline{[(\bar{z}+\alpha(-\bar{x}))(\bar{z}+\overline{\alpha(-x)})]} \ . \tag{89}$$

The proof follows from equating coefficients of linear and free terms (in z). □

Remark 6.4. It is easy to verify using the moment conditions for $\alpha(x)$ from [24] that odd $\alpha(x)$ would imply $w(0) = 0$ and

$$\int_{-\infty}^{\infty} \frac{w'(\zeta)}{|\zeta|} d\zeta = 0 \ . \tag{90}$$

Equation (88) obviously implies

$$R(-\bar{x},-\bar{z}) = \pm\overline{R(x,z)} \ . \tag{91}$$

Based on our choice of the branchcut of R, it is clear that in the case of real x, z the sign in (91) is positive if $|z| < \mu_+$ and negative if $|z| > \mu_+$. In the case $x \in R$ the branchcut $\gamma(x)$ is

symmetrical with respect to $\mathbb{R}$ and intesect $\mathbb{R}$ only at $z = \mu_+$. If $x \in \mathbb{R}$ and $\Im z > 0$, the sign in (91) is positive only if there exists a curve $\sigma(z)$ connecting z with the origin, such that $\sigma(z) \cap \gamma(x) = \emptyset$ and simultaneously $-\overline{\sigma(z)} \cap \gamma(-\bar{x}) = \emptyset$. It is clear that if such $\sigma(z)$ does not exist then $\sigma(z)$ can be choosen in such a way that $\sigma(z) \cap \gamma(x) = \emptyset$ and $-\overline{\sigma(z)}$ intersects $\gamma(-\bar{x})$ only one time. Then the sign in (91) is negative. In the case of a complex $x \in \mathcal{B}$ the sign in (91) is defined as above.

Let $\Sigma_*(x)$ denote the region (not necessarily simple) bounded by the curve $\gamma(-\bar{x}) \cup \{-\overline{\gamma(x)}\}$, and let $\Sigma(x) = (\Sigma_*(x) \cup \{-\overline{\Sigma_*(x)}\} \cap \bar{\mathbb{C}}^+$. Clearly, $\Sigma(x)$ is symmetrical with respect to imaginary axis and has the segment $[-\mu_+, \mu_+]$ a its lower boundary. Then, for every $x \in \mathcal{B}$, equation (88) has positive sign if $z \in \Sigma(x)$ and negative sign if $z \notin \Sigma(x)$.

Theorem 6.5. *If* $\alpha(-\bar{x}) = -\overline{\alpha(x)}$ *then*

$$h(-\bar{x}, -\bar{z}) = \mp\overline{h(x, z)} \ , \tag{92}$$

where the sign is negative if $z \in \Sigma(x)$ *and positive otherwise. Conversly,* (92) *implies that* $\alpha(x)$ *is odd or* $\alpha(-\bar{x}) = -\overline{\alpha(x)}$.

Proof. According to (50) and to Statements 6.2, 6.3,

$$h(-\bar{x}, -\bar{z}) = \int_{-\bar{x}}^{-\overline{x(z)}} R(u, -\bar{z})du = -\int_x^{x(z)} R(-\bar{y}, -\bar{z})d\bar{y} = \mp\int_x^{x(z)} \overline{R(y, z)dy} = \mp\overline{h(x, z)} \ , \tag{93}$$

where $y = -\bar{u}$. The last to terms of (93) have sign minus if $z \in \Sigma(x)$ and sign plus if $z \notin \Sigma(x)$.

To prove the converse, we need to show that (93) implies (88). Let us choose some $x = iy,\ y \in \mathbb{R}$, $z \in \Sigma(x)$ and let us introduce

$$m(y, z) = -ih(iy, z) = -ih(x, z) \ . \tag{94}$$

Then

$$h(-\bar{x}, -\bar{z}) = h(i\bar{y}, -\bar{z}) = im(\bar{y}, -\bar{z}) \quad -\overline{h(x, z)} = i\overline{m(y, z)} \ , \tag{95}$$

so, according to (93),

$$m(\bar{y}, -\bar{z}) = \overline{m(y, z)} \ . \tag{96}$$

Since m is analytic in y, we have Taylor expansion $m(y, z) = \sum_{k=0}^{\infty} a_k(z)y^k$, so that (96) is equivalent to

$$\overline{a_k(z)} = a_k(-\bar{z}) \qquad\qquad \forall k \in \mathbb{N} \ . \tag{97}$$

Since $m_y(y, z) = \sum_{k=1}^{\infty} ka_k(z)y^{k-1}$ has Taylor coefficients satisfying (97), we obtain

$$m_y(\bar{y}, -\bar{z}) = \overline{m_y(y, z)} \ . \tag{98}$$

But $m_y(y, z) = h_x(iy, z) = h_x(x, z) = -R(x, z)$. Thus, (98) implies (91) with positive sign. By analyticity of h, this result can be extended from purely imaginary to all x. Similarly, we can obtain (91) with negative sign when $z \notin \Sigma(x)$. Thus, (92) implies (88). Statement 6.3 completes the proof. □

Corollary 6.6. *In the case $x, z \in \mathbb{R}$ equation* (92) *implies that $w(z) = \operatorname{sign}(z-\mu_+)\Im h(x,z)$ is an even function and*

$$\begin{aligned} \Re h(-x,-z) &= -\Re h(x,z) \quad \text{if} \quad |z| < \mu_+ \\ \Re h(-x,-z) &= \Re h(x,z) \quad \text{if} \quad |z| > \mu_+ \ . \end{aligned} \tag{99}$$

Corollary 6.6 states that $\Im h(x,z)$ is even on $z \in [-\mu_+, \mu_+]$ and is odd outside $[-\mu_+, \mu_+]$. Therefore, $h_z(x,z)$ is odd on $z \in [-\mu_+, \mu_+]$ and is even outside $[-\mu_+, \mu_+]$. Taking into account Remark 6.4 and Statement 6.1, we obtain the following corollary.

Corollary 6.7. *If $\Im h(0,0) \neq 0$ then* (92) *implies that the initial potential $q(x,0)$ is an even function.*

Given a scattering data (see [24]), we know $w(z)$ but not necessarily $h(x,z)$. So, does even $w(z)$ implies even $q(x,0)$ under the inverse scattering procedure of [22], [24]? According to (50), $h(x,z)$ depends on the branchcut of $R(x,z)$. Let us denote by R_R, R_L and h_R, h_L the radical $R(x,z)$ (and corresponding to it $h(x,z)$) with the branchcut passing through $\pm\mu_+$ respectively (in the case of even $w(z)$ we have $\mu_- = -\mu_+$). In all the statements above, we considered $R = R_R$ and $h = h_R$. In the case of $x, z \in \mathbb{R}$ we choose $R_L(x,z)$ to be positive for $z > -\mu_+$ and preserve the orientation of contour γ^+ (from μ_+ to $-\mu_+$) in the matrix RHP for the inverse scattering transform. With such choice of R_L, it follows from (50) that $h_L(x,z) = \pm h_R(x,z)$ for $x, z \in \mathbb{R}$ and $|z| < \mu_+$ or $|z| > \mu_+$ respectively. If $\alpha(x)$ satisfies (86), then, according to Theorem 6.5, $h_L(-\bar{x}, -\bar{z}) = h_R(-\bar{x}, -\bar{z}) = -\overline{h_R(x,z)}$ for $z \in \Sigma(x)$ and $h_L(-\bar{x}, -\bar{z}) = -h_R(-\bar{x}, -\bar{z}) = -\overline{h_R(x,z)}$ for $z \notin \Sigma(x)$. For $x \in \mathbb{R}$ that means

$$\Im h_L(-x, -\bar{z}) = \Im h_R(x,z) \tag{100}$$

for all z. Thus, we can formulate a stronger version of Corollary 6.7.

Corollary 6.8. *If $w(z)$, $z \in \mathbb{R}$, is even and if for all $x \geq 0$ the inverse scattering procedure of [22], [24] produces a semiclassical solution* (7) *with $a(x) = -\frac{1}{2}S'(x)$ and $b(x) = A(x)$, such that $\alpha(x)$ is analytic in a region containg $x \geq 0$ and satisfies* (86) *in a vicinity of $x = 0$, then $q(x,0)$, evenly continued to the whole $\mathbb{R}$, is the initial potential corresponding to the scattering data $w(z)$ according to the procedure of [22], [24].*

Proof. Let $\alpha(x)$, $x \geq 0$, be solution of the modulation equations (moment conditions), expressed in terms of $w(z)$, see [24], Sect. 3.1.1. By Remark 3.1 of [24], $\alpha(x) = -\overline{\alpha(-x)}$ satisfies modulation equations when $x < 0$. Thus, we can assume that $\alpha(x)$, $x \in \mathbb{R}$, is analytic on $\mathbb{R}$ and satisfies (86). According to Theorem 6.5, the corresponding h_R and h_L satisfy (92). By the assumption, the main and complementary arcs have the required distribution of signs of $\Im h_R(x,z)$ for all $x \geq 0$. Then, according to (100), in the case of $x < 0$ the main and complementary arcs have the required distribution of signs of $\Im h_L(x,z)$. Thus, the initial data represented by $\alpha(x)$, $x \in \mathbb{R}$, indeed corresponds to the given scattering data $w(z)$ through the inverse scattering procedure of [22], [24]. □

7 Examples

7.1 Example of [22], $\mu = 2$

The case of

$$a(x) = \frac{\mu}{2}\tanh x,\ b(x) = \text{sech }(x), \tag{101}$$

$\mu > 0$, was studied in details in [22]. The leading order (in ε)

$$f_0(z) = \lim_{\varepsilon\to 0}\frac{i\varepsilon}{2}\ln r_{init}(z,\varepsilon)\ , \tag{102}$$

where $r_{init}(z,\varepsilon)$ is the reflection coefficient of Zakharov-Shabat problem for the focusing NLS with the inital data (7), $A(x) = b(x)$ and $-\frac{1}{2}S'(x) = a(x)$, is calculated there to be

$$\begin{aligned} f_0(z) =&(\frac{\mu}{2} - z)\left[\frac{i\pi}{2} + \ln(\frac{\mu}{2} - z)\right] + \frac{z+T}{2}\ln(z+T) + \frac{z-T}{2}\ln(z-T) \\ &- T\tanh^{-1}\frac{T}{\frac{\mu}{2}} + \frac{\mu}{2}\ln 2 + \frac{\pi}{2}\varepsilon, \qquad \text{when } \Im z \geq 0, \end{aligned} \tag{103}$$

where $T = \sqrt{\frac{\mu^2}{4} - 1}$. This calculation involved exact solution of Zakharov-Shabat problem in terms of hypergeometric functions, followed by Stirling's asymptotic formula. Note that $f_0(z)$ has a log point $T \in \mathcal{E}$ in the case $\mu < 2$ and has no log points in $\mathcal{E}$ in the case $\mu \geq 2$. This is the reflection of the fact that the initial data (101) is purely radiative in the case $\mu \geq 2$, and contains points of the descrete spectrum (solitons) on the vertical segment $[-T, T]$ in the case $\mu < 2$ (see [20]). From (103) one readily obtain

$$f_0'(z) = -\frac{i\pi}{2} - \ln(\frac{\mu}{2} - z) + \frac{1}{2}\ln(z^2 - T^2)\ , \tag{104}$$

and

$$w'(z) = -\frac{\pi}{2}\text{sign}z\left(1 - \chi_{[-T,T](z)}\right),\ z \in \mathbb{R}. \tag{105}$$

Since the asymptotic inverse scattering transform, developed in [22], [24], uses only the values $w'(z),\ z \in \mathbb{R}$, and, in the case $\mu < 2$, the jump of $f_0'(z)$ over the slit $[0, T]$, we will focus on calculating these quantitees.

Consider first the simplest case $\mu = 2$. Then $\mu_\pm = \pm 1$,

$$\alpha(x) = \frac{\sinh x + i}{\cosh x}, \qquad \tilde{\alpha}(x) = \frac{\sinh x - i}{\cosh x} \tag{106}$$

and

$$\alpha'(x) = \frac{1 - i\sinh x}{\cosh^2 x}\ . \tag{107}$$

According to (106), $\alpha(x)$ is a meromorphic function with poles at $\frac{i\pi}{2} + 2\pi i m$ and zeroes at $-\frac{i\pi}{2} + 2\pi i m$, $m \in \mathbb{Z}$. Since

$$\alpha(\xi \pm \frac{i\pi}{2}) = \frac{\cosh\xi \pm 1}{\sinh\xi}\ , \tag{108}$$

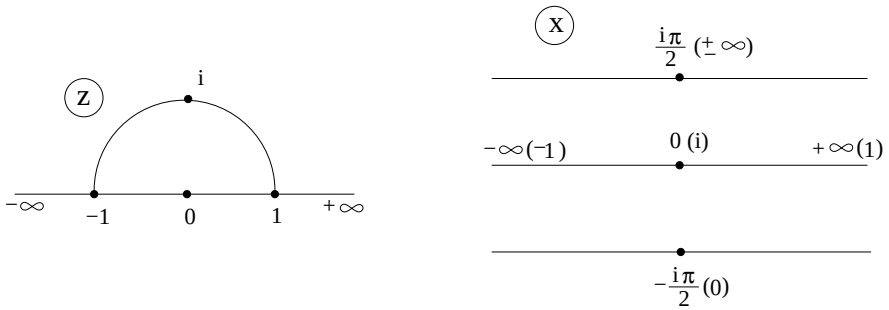

Figure 12: The strip $\mathcal{B} = \{x : \ -\frac{\pi}{2} \le \Im x \le \frac{\pi}{2}\}$ is mapped onto the upper half plane of z-plane by $z = \alpha(x)$, so that $\alpha(\mathcal{B}^-) = \mathcal{E}^+$. Shown in parentheses are the corresponding images of the map $\alpha(x)$, i.e., the preimages of the inverse to $\alpha(x)$ map $x(z)$.

we see that $\mathcal{B}$ is the strip $-\frac{\pi}{2} \le \Im x \le \frac{\pi}{2}$, where $\frac{i\pi}{2} = x(\pm\infty)$, $-\frac{i\pi}{2} = x(0)$ and $\pm\infty = x(\pm 1)$ respectively, see Fig 12. Since $\alpha'(x) \neq 0$ inside $\mathcal{B}$, there are no branchpoints in $\mathcal{B}$. Note that for all $x \in \mathbb{R}$ we have

$$a^2(x) + b^2(x) = 1 \ , \tag{109}$$

so that $\mathcal{E}$ is the unit disc.

In the case $\mu = 2$, the inverse function $x(z)$ to $\alpha(x)$ on $\mathbb{C}^+$ is very simple. In order to find it, we calculate

$$(z - \alpha)(z - \tilde{\alpha}) = (z - a)^2 + b^2 = z^2 - 2az + 1 = 0 \ , \tag{110}$$

which yields solution $a(z) = \frac{1}{2}[z + \frac{1}{z}]$. (Here we use notation $a(z)$ for $a(z) = a(x(z))$.) Thus

$$x(z) = \tanh^{-1} a(z) = \tanh^{-1} \frac{1}{2}[z + \frac{1}{z}] \ . \tag{111}$$

According to (71), we have

$$w(z) = \mathrm{sign}(1-z)\Im \int_{x(z)}^{x} \sqrt{z^2 - 2z\tanh y + 1}dy = \mathrm{sign}(1-z)\Im \int_{a(z)}^{\tanh x} \sqrt{z^2 - 2z\eta + 1}\frac{d\eta}{1-\eta^2} \ , \tag{112}$$

where $z \in \mathbb{R}$, $x \in \mathbb{R}$ is arbitrary and $y = \tanh^{-1}\eta$. Let us consider the case $z > 0$. Then $a(z) > 1$, so the contour of integration in the latter integral is along the real segment $[\tanh x, a(z)]$ of the complex η-plane (complex a-plane), except the singular point $\eta = 1$, which is traversed from above or from below if $z > 1$ or $z < 1$ respectively, see Fig. 13. Since the integrand is real on $\mathbb{R}$, only integration around $\eta = 1$ contribute to the imaginary part of the integral. Thus

$$w(z) = \pi i \ \mathrm{Res} \ \frac{\sqrt{z^2 - 2z\eta + 1}}{1 + \eta}\bigg|_{\eta=1} = \frac{i\pi}{2}(1 - z) \ , \tag{113}$$

where the square root is choosen positive when $z < 1$ and negative when $z > 1$ respectively. By similar argument (but without $\mathrm{sign}(1 + z)$ involved), we obtain

$$w(z) = \frac{i\pi}{2}(1 + z) \tag{114}$$

Figure 13: Upper contour of integration is for $z > 1$, lower - for $z < 1$.

for $z < 0$. Thus, $w(z)$ obtained through (71) with initial data from (110) coincides with $\Im f_0(z),\ z \in \mathbb{R}$, where f_0 is given by (103) with $\mu = 2$ (and $T = 0$). The correct distribution of signs of $\Im h(x, z)$ along the main and complementary arcs (inequality (27)) follows directly from the analysis of zero level curves of $\Im h(x, z)$ with a fixed $x \in \mathbb{R}$ in the upper z-halfplane (three zero level curves entering $\mathbb{C}^+$ at ± 1 and ∞ respectively meet at the branchpoint $\alpha(x)$). One can also observe that $f_0(z)$ given by (103) can be obtained through the Cauchy transform of $w(z)$ (see [24]), and that sign distribution (27) for this $f_0(z)$ was proven in [22].

7.2 Example of [22], general case

We consider now the general case $\mu > 0$ in (101). Then (106) - (110) become

$$\begin{gathered}
\alpha(x) = \frac{\frac{\mu}{2}\sinh x + i}{\cosh x}, \qquad \tilde{\alpha}(x) = \frac{\frac{\mu}{2}\sinh x - i}{\cosh x}, \\
\alpha'(x) = \frac{\frac{\mu}{2} - i\sinh x}{\cosh^2 x}, \qquad \alpha(\xi \pm \frac{i\pi}{2}) = \frac{\frac{\mu}{2}\cosh\xi \pm 1}{\sinh\xi}, \\
\frac{4}{\mu^2}a^2(x) + b^2(x) = 1, \\
(z-\alpha)(z-\tilde{\alpha}) = (z-a)^2 + b^2 = z^2 - \mu z\tanh x + 1 + T^2\tanh^2 x = 0
\end{gathered} \tag{115}$$

respectively. The latter equation implies

$$\tanh x(z) = \frac{\frac{\mu}{2}z \pm \sqrt{z^2 + \left(1 - \frac{\mu^2}{4}\right)}}{\frac{\mu^2}{4} - 1}\ , \tag{116}$$

where the correct branch of the radical in the right hand side should be chosen. Equations (115) show that $\mathcal{E}$ is the ellipse centered at $z = 0$ with horizontal and vertical semiaxes $\frac{\mu}{2}$ and 1 respectively. The complement of $\mathcal{E}^+$ in $\mathbb{C}^+$ is mapped onto the strip $0 \le \Im x \le \frac{\pi}{2}$ in the x-plane.

To find the image of $\mathcal{E}^+$, we need to study the branchpoints x^* of $x(z)$ defined by

$$\sinh x^* = -\frac{\mu}{2}i\ . \tag{117}$$

The images of branchpoints in z-plane (log points), obtained by substituting (117) into the expression for $\alpha(x)$, are

$$z^* = \pm\sqrt{\frac{\mu^2}{4} - 1} = \pm T\ . \tag{118}$$

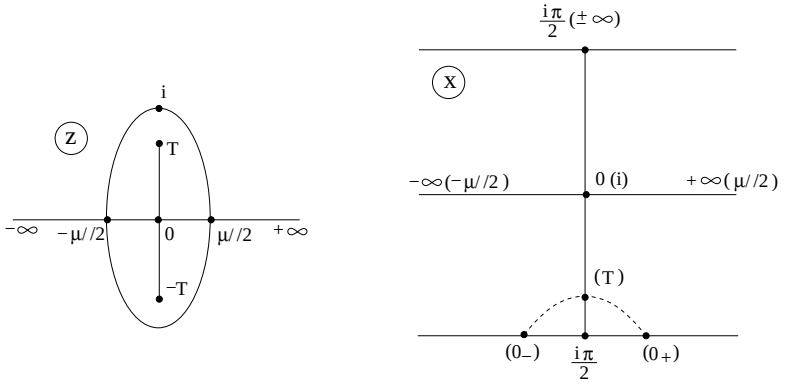

Figure 14: Mapping $\alpha(x)$, case $\mu < 2$. Shown in parentheses are the corresponding images of the map $\alpha(x)$, i.e., the preimages of the inverse to $\alpha(x)$ map $x(z)$. Set $\mathcal{B}$ is the strip $\{x:\ -\frac{\pi}{2} \le \Im x \le \frac{\pi}{2}\}$ without the region bounded by the dashed contour, which is the image of two sides of the slit $[0, T]$ by the map $x(z)$.

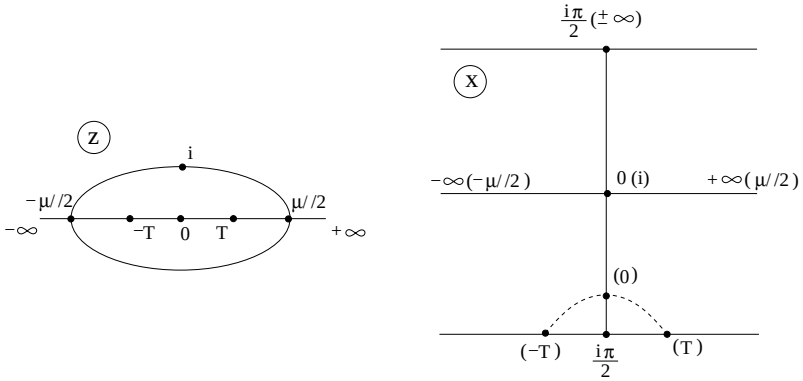

Figure 15: Mapping $\alpha(x)$, case $\mu > 2$. Shown in parentheses are the corresponding images of the map $\alpha(x)$, i.e., the preimages of the inverse to $\alpha(x)$ map $x(z)$. Set $\mathcal{B}$ is the strip $\{x:\ -\frac{\pi}{2} \le \Im x \le \frac{\pi}{2}\}$ without the region bounded by the dashed contour, which is the image of the segment $[-T, T]$ by the map $x(z)$.

In the case $\mu > 2$ log points $\pm T \in (-\frac{\mu}{2}, \frac{\mu}{2})$ are not in the upper halfplane. In the case $\mu < 2$ log points $\pm T = \pm i|T|$. In the latter case, we make a branchcut of $x(z)$ in $\mathbb{C}^+$ over the segment $[0, T]$. It is now easy to find the image $\mathcal{B}^-$ of the region $\mathcal{E}^+$ (with the cut if $\mu < 2$), see Fig. 14, Fig. 15 for $\mu < 2,\ \mu > 2$ respectively. Equations of the arc, connecting points $x(0^\pm)$ and $x(T)$, case $\mu < 2$, and $x(\pm T)$ and $x(0)$, case $\mu > 2$, are obtained from conditions $\Re\alpha(y) = 0$ and $\Im\alpha(y) = 0$ respectively. These equations are

$$-\sin\eta = \frac{\mu}{2}\cosh\xi \quad \text{and} \quad \cosh\xi = \frac{\mu}{2}\sin\eta \tag{119}$$

respectively, where $y = \xi + i\eta$.

Let us now calculate $w(z)$, $z \in \mathbb{R}$, for the case $\mu > 2$ (we only consider $|z| > T$) or for the case $\mu < 2$. Using (115), we obtain direct and inverse maps between the values of a and

z by

$$z = a + i\sqrt{1 - \frac{4}{\mu^2}a^2}, \qquad a = \frac{\frac{\mu}{2}z - \sqrt{z^2 - T^2}}{T^2} \cdot \frac{\mu}{2} \tag{120}$$

The latter maps $\mathcal{E}^+$ into a part of the lower a-halfplane and $\mathbb{C}^+ \setminus \mathcal{E}$ into the upper a-halfplane, see Fig. 16, Fig. 17. Using (120), it is easy to check that if $z \geq T$, $\mu > 2$ or $z \geq 0$, $\mu < 2$, then the corresponding $a = \hat{a}(z) = a(x(z)) \in \mathbb{R}$ and $a > \frac{\mu}{2}$. Making change of variables $a(y) = \eta$ in

$$w(z) = \operatorname{sign}(\frac{\mu}{2} - z)\Im \int_{x(z)}^{x} \sqrt{(z - a(y))^2 + b^2(y)}dy \tag{121}$$

and using (115), we obtain

$$\begin{aligned} w(z) =& \operatorname{sign}(\frac{\mu}{2} - z)\Im \int_{a(x(z))}^{a(x)} \sqrt{(z-\eta)^2 + 1 - \frac{4\eta^2}{\mu^2}} \cdot \frac{d\eta}{\frac{\mu}{2}\left(1 - \frac{4\eta^2}{\mu^2}\right)} \\ =& \operatorname{sign}(\frac{\mu}{2} - z)\Im \int_{a(x(z))}^{a(x)} \sqrt{\frac{\mu^2}{4}(z-\eta)^2 + \frac{\mu^2}{4} - \eta^2} \cdot \frac{d\eta}{\frac{\mu^2}{4} - \eta^2} \ . \end{aligned} \tag{122}$$

Direct calculation show that the integrand is real-valued. Thus, a contribution to the imaginary part of the latter integral can come only from integration around the singular point $\eta = \frac{\mu}{2}$. Repeating the previous argument (case $\mu = 2$), we obtain

$$w(z) = \frac{\pi}{2}(\frac{\mu}{2} \mp z) \tag{123}$$

if $\operatorname{sign} z = \pm 1$ respectively. Using the above technique, one could check that in the case $\mu > 2$, $w(z)$ should be constant on the segment $[-T, T] \subset \mathbb{R}$. Thus, $w(z)$ satisfies the inequalities (26) for all $\mu > 0$. In the pure radiational case $\mu > 2$, the proof of the sign distribution (27) is the same as for the case of $\mu = 2$ in Section 7.1. This proof can be extended to the case $m < 2$ providing that the contour γ does not intersect the branchcut of $f_0(z)$. However Lemma 4.11 from [22] shows that $\gamma_m = \gamma_m(x)$, which is defined by $f_0(z)$ given by (103), intersects the branchcut $[0, T]$ if x is negative with sufficiently large $|x|$. In this case one can use Corollary 6.8 from Section 6 to show that $q_0(x, 0, \varepsilon)$ is $O(\varepsilon)$ close to $\tilde{q}(x, 0, \varepsilon)$ for all $x \in \mathbb{R}$.

wzmgenpm

Let us now calculate the jump

$$\Delta f(z) = f(x, z_-) - f(x, z_+) = h(x, z_+) - h(x, z_-) \tag{124}$$

for the case $0 < \mu < 2$, where the points $z_\pm$ are equal but located on the opposite shores of the oriented vertical segment $[T, 0]$. According to (50), we have

$$\Delta f(z) = \int_{x(z_-)}^{x(z_+)} \sqrt{(z - a(y))^2 + b^2(y)}dy \tag{125}$$

where $x(z_-), x(z_+)$ are symmetrically located points on the dashed curve, Fig. 14. Using the change of variables $\eta = \tanh x$, we obtain

$$\Delta f(z) = \int_{\eta_-}^{\eta_+} \sqrt{z^2 - \mu z\eta + 1 + T^2\eta^2} \cdot \frac{d\eta}{1 - \eta^2} \ , \tag{126}$$

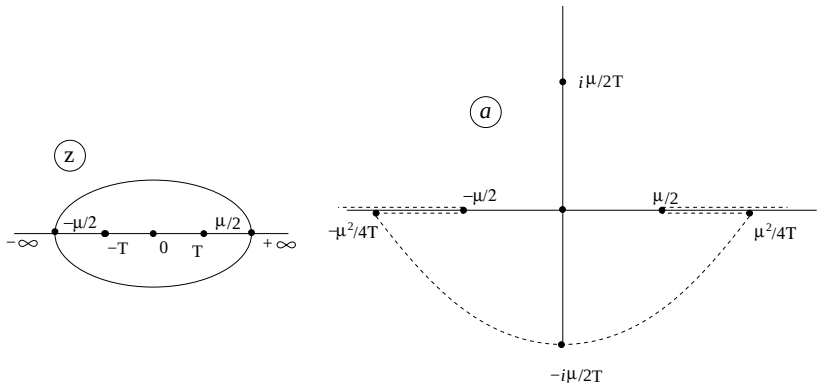

Figure 16: Mappings (120) in the case $\mu > 2$. The dashed line in the a-plane is the image of $\mathbb{R}$ by the map $\hat{a}(z) = a(x(z))$. In particular, $\hat{a}(\pm\infty) = \pm\infty$, $\hat{a}(\pm\frac{\mu}{2}) = \pm\frac{\mu}{2}$, $\hat{a}(\pm T) = \pm\frac{\mu^2}{4T}$, $\hat{a}(0) = -\frac{i\mu}{2T}$.

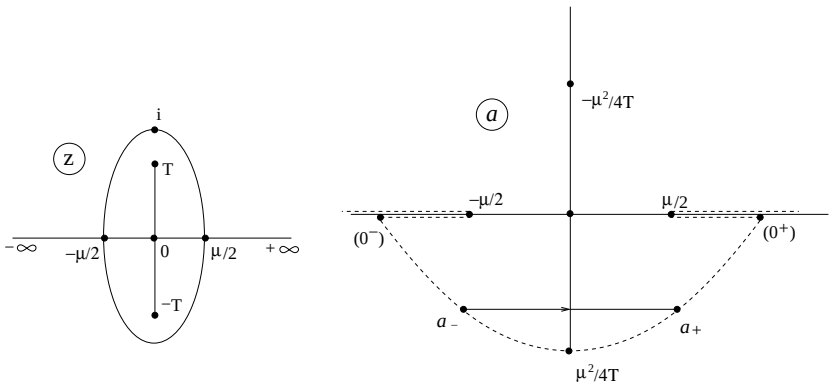

Figure 17: Mappings (120) in the case $\mu < 2$. The dashed line in the a-plane is the image of $\mathbb{R}$ by the map $\hat{a}(z) = a(x(z))$. In particular, $\hat{a}(\pm\infty) = \pm\infty$, $\hat{a}(\pm\frac{\mu}{2}) = \pm\frac{\mu}{2}$, $\hat{a}(0^{\pm}) = \pm\frac{\mu}{2T}$, $\hat{a}(T) = \frac{\mu^2}{4T}$. The solid line shows the contour of integration from a_- to a_+.

where, according to (120),

$$\eta_\pm = \frac{\frac{\mu}{2}z \pm \sqrt{z^2 - T^2}}{T^2} = \frac{\frac{\mu}{2}iy \pm \sqrt{-y^2 - T^2}}{T^2} \tag{127}$$

with $z = iy$, see Fig. 17, where $a_\pm = \frac{\mu}{2}\eta_\pm$.

Observing that $\eta_\pm$ are zeroes of the radical in (126), we obtain

$$\Delta f(z) = \frac{1}{2}\int_\lambda \sqrt{z^2 - \mu z\eta + 1 + T^2\eta^2}\cdot\frac{d\eta}{1-\eta^2}\ , \tag{128}$$

where $\lambda \subset \mathbb{C}^-$ is a closed, clockwise oriented curve that contains the segment $[\eta_-, \eta_+]$. Thus,

$$\begin{aligned}\Delta f(z) &= -\frac{i\pi}{2}\left[\text{Res }\sqrt{z^2 - \mu z\eta + 1 + T^2\eta^2}\,\Big|_\infty \pm \text{Res }\sqrt{z^2 - \mu z\eta + 1 + T^2\eta^2}\Big|_{\eta=\pm1}\right] \\ &= \frac{i\pi}{2}\left[\sqrt{z^2 - \mu z + \frac{\mu^2}{4}} - \sqrt{z^2 + \mu z + \frac{\mu^2}{4}} - 2T\right] = i\pi(z - T)\ .\end{aligned} \tag{129}$$

Thus, we obtained the same value of $\Delta f(z)$ as (103) has. It is now possible to reconstruct $f_0(z)$, given by (103) with $\mu < 2$, from $w(z)$ defined by (123) and $\Delta f(z)$ defined by (129) on $[0, T]$.

7.3 The "Y" - shape of Bronski

In [2], J. Bronski studied numerically discrete spectrum of ZS problem (1) with the potential $q(x, 0\varepsilon)$ given by (7), where

$$A(x) = \text{sech }2x, \qquad S(x) = \mu\text{sech }2x. \tag{130}$$

He found that for real valued $q(x, 0\varepsilon)$, i.e., for $\mu = 0$, the accumulation curve for discrete eigenvalues of (1), (130) in $\mathbb{C}^+$ in the limit $\varepsilon \to 0$ is a segment $[0, i]$ of the imaginary axis. In the case $\mu = 1$, the accumulation curve has "Y" - shaped form, with $z = 0$ located at the bottow of "Y". The change of shape of the accumulation curve happens at the critical value $\mu^* = 2^{-\frac{3}{2}}$. In this section we show that the endpoints of the accumulation curve coicide with the branchpoints of $f_0(z)$, obtained from the potential (7), (130) by the AH transformation (24). In particular, μ^* is a critical value when one branchpoint of $f_0(z)$ splits into two.

For potential (7), (130), we have

$$\alpha(x) = \frac{\mu\sinh 2x}{\cosh^2 2x} + \frac{i}{\cosh 2x} = \frac{\mu\sinh 2x + i\cosh 2x}{cosh^2 2x}\ . \tag{131}$$

Then

$$\alpha'(x) = 2\mu\frac{\cosh^2 2x - 2\sinh^2 2x}{\cosh^3 2x} - 2i\frac{\sinh 2x}{\cosh^2 2x} = -\frac{\mu\cosh 4x + i\sinh 4x - 3\mu}{\cosh^3 2x}\ , \tag{132}$$

so, after some algebra, equation $\alpha'(x) = 0$ for the branchpoints can be written as

$$(\mu + i)e^{8x} - 6\mu e^{4x} + \mu - i = 0\ . \tag{133}$$

Solution of (133) is given by

$$\left(e^{4x}\right)_{1,2} = \frac{3\mu \pm \sqrt{8\mu^2 - 1}}{\mu + i} \ . \tag{134}$$

Thus, for $\mu = 0$ we obtain $e^{4x} = 1$, so $x = 0$ is a branchpoint and $z = \alpha(0) = i$ is the corresponding log point in the spectral plane.

The critical value μ^* is given by equation $8\mu^2 - 1 = 0$, which yields $\mu^* = 2^{-\frac{3}{2}}$. For $\mu \le \mu^*$, direct calculation show that $|e^{4x}| = 1$ for solution e^{4x} given by (134) with the positive sign. Thus, the corresponding log point $x \in \imath R$. Substituting μ^* into (134), we find $e^{4x^*} = \frac{1}{3}(1 - 2\sqrt{2}i)$, where $x^* = -\frac{i}{2}\tan^{-1}(2\sqrt{2})$ is the the branchpoint that corresponds to μ^*. Direct calculations show that the corresponding log point on the spectral plane (the double point on Fig. 11 in [2]) is given by $z^* = \alpha(x^*) = i\frac{3\sqrt{3}}{4\sqrt{2}} \approx 0.91856i$.

To calculate the log point(s) (endpoint(s) of the accumulation curve) for other values of μ, we rewrite (133) as

$$(\mu^2 + 1)\cosh^2 4x - 6\mu^2 \cosh 4x + 9\mu^2 - 1 = 0 \ , \tag{135}$$

which yields

$$(\cosh 4x)_{1,2} = \frac{3\mu^2 \pm \sqrt{1 - 8\mu^2}}{\mu^2 + 1} \ . \tag{136}$$

Substituting $\mu = 0$, we see that for $\mu < \mu^*$ we need to choose the positive sign in (136). Calculating now $\cosh 2x$ and $\sinh 2x$, we can express logpoints $\alpha(x)$ for an arbitrary $\mu > 0$ as

$$\alpha(x) = \frac{-\mu\sqrt{2\mu^2 - 1 \pm \sqrt{1 - 8\mu^2}} + i\sqrt{4\mu^2 + 1 \pm \sqrt{1 - 8\mu^2}}}{4\mu^2 + 1 \pm \sqrt{1 - 8\mu^2}} \cdot \sqrt{2(\mu^2 + 1)} \ , \tag{137}$$

were only the plus sign should be used for $\mu < \mu^*$ (note the choice of signs for the radicals representing $\cosh 2x$ and $\sinh 2x$).

Expression (137) provides the endpoints of the two "legs" of the "Y"-shaped accumulation curve (as $\varepsilon \to 0$) for the points of the discrete spectrum in the case $\mu > \mu^*$. In the case $0 \le \mu \le \mu^*$, it gives the tip of the vertical segment on the imaginary axis where the points of the discrete spectrum accumulate.

7.4 Double hump initial data

Another example of an interesting initial data is

$$a(x) = \tanh x, \ b(x) = \text{sech } x - k\text{sech }^2 x, \quad k \in [0, 1], \tag{138}$$

which contains double hump cases. Indeed, if $k > \frac{1}{2}$, then $b = u - ku^2$, where $u = \text{sech } x$, has a global maximum at $u = 1/2k \in (0, 1)$. So, $x = \pm\cosh^{-1}(2k)$ are two points of maximum of $b(x)$.

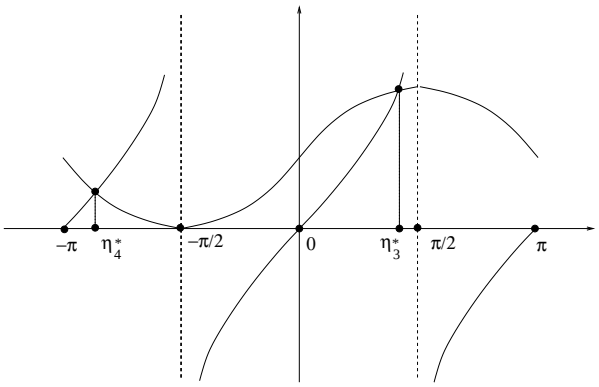

Figure 18: Intersections of functions $1+\sin\eta$ and $2k\tan\eta$ and points $\eta^*_{3,4}$.

The points of ramification of the map

$$\alpha(x)=\tanh x+i(\text{sech }x-k\text{sech }^2x) \quad \text{with} \quad \alpha'(x)=\frac{1-i\sinh x+2ik\tanh x}{\cosh^2 x} \tag{139}$$

satisfy equation

$$1-i\sinh x+2ik\tanh x=0. \tag{140}$$

Coefficients of this equation are $2\pi i$ periodic functions. The substitution $u=\sinh x$ in (140) yields a forth order polinomial equation in u. Thus, there are no more than 4 ramification points of $\alpha(x)$ within a horizontal strip of width 2π in the complex x-plane.

Separating real and imaginary parts of (140), we obtain the system

$$\begin{cases} \frac{1}{2}\sinh(2\xi)\cos(2\eta)-2k\sinh\xi\cos\eta-\sinh\xi\sin\eta=0 \\ \frac{1}{2}\cosh(2\xi)\sin(2\eta)-2k\cosh\xi\sin\eta+\cosh\xi\cos\eta=0, \end{cases} \tag{141}$$

where $x=\xi+i\eta$. The first equation in (141) has a common factor $\sinh\xi$. Setting it zero, we obtain $\xi=0$. Then the second equation (141) becomes $1+\sin\eta=2k\tan\eta$. Fig. 18 shows that this equation has one positive solution η^*_3 and one negative solution η^*_4 on $(-\pi,\pi)$, where $0<\eta^*_3<\frac{\pi}{2}$ and $\eta^*_4<-\frac{\pi}{2}$. We denote by $x^*_{3,4}$ the corresponding ramification points in the complex x-plane.

Considering $\xi\neq 0$, we rewrite the first equation in (141) as

$$\cosh\xi\cos(2\eta)-2k\cos\eta-\sin\eta=0, \tag{142}$$

which yields

$$\cosh\xi=\frac{\sin\eta+2k\cos\eta}{\cos(2\eta)}\ . \tag{143}$$

Substitution of (143) into the second equation of (141) yields

$$\cosh^2\xi=\frac{1}{2}\frac{(4k^2-1)\sin(2\eta)-2k\cos(2\eta)+\frac{1}{2}\sin(2\eta)\cos(2\eta)}{\sin(2\eta)\cos(2\eta)}\ . \tag{144}$$

From (151)-(144) after some algebra we obtain

$$u^3+4k^2u+4k=0, \tag{145}$$

where $u = \sin(2\eta)$. Equation (145) should yield the remaining two points of ramification. In the case $k = \frac{1}{2}$ equation (145) becomes $(u+1)[u^2 - u + 2] = 0$, which has the only real root $u = -1$. Substituting the corresponding $\eta = -\frac{\pi}{4}$ into the second equation of (141), we obtain $\cosh 2\xi = 2\sqrt{2\cosh\xi}$, or $\xi = \pm\cosh^{-1}\left(1 + \frac{1}{\sqrt{2}}\right)$. Thus, for $k = \frac{1}{2}$ we obtain the remaining ramification points

$$x^*_{1,2} = \pm\cosh^{-1}\left(1 + \frac{1}{\sqrt{2}}\right) - \frac{i\pi}{4} \ . \tag{146}$$

It is clear that in the case of arbitrary $k \geq 0$ equation (145) has only one real solution. Indeed, if that is not the case, then (145) would have a multiple real root for some $k > 0$. But equation $m'(u) = 3u^2 + k^2 = 0$, where $m(u) = u^3 + 4k^2u + 4k$ has no real roots, so there is a unique real root $u(k)$ of (145). Moreover, $u(k) \in (0, -1]$, since $m(0) > 0$ and $m(-1) \leq 0$. Thus, $\eta = \frac{1}{2}\sin^{-1}u(k)$ or $\eta = -\frac{\pi}{2} - \frac{1}{2}\sin^{-1}u(k)$. Substituting one of these values into (143) (the former if $k \geq \frac{1}{2}$ and the latter if $k \leq \frac{1}{2}$), we find the real components of the two remaining points of ramification $x^*_{1,2}$. Note that $\Re x^*_1 = -\Re x^*_2$.

To calculate the pre-images of $z = 0$ of the map (139), we set equation

$$z\cosh^2 x = \sinh x\cosh x + i\cosh x - ik \ . \tag{147}$$

For the same reasons as above, for every $z \in \overline{\mathbb{C}^+}$ this equation has four roots in the strip $-\pi < \Im x \leq \pi$. Assuming $z \in \mathbb{R}$ and separating real and imaginary parts of (147), we obtain

$$\begin{cases} z(\cosh(2\xi)\cos(2\eta) + 1) = \sinh(2\xi)\cos(2\eta) - 2\sinh\xi\sin\eta \\ z(\sinh(2\xi)\sin(2\eta) = \cosh(2\xi)\sin(2\eta) + 2\cosh\xi\cos\eta - 2k \ . \end{cases} \tag{148}$$

If $z = 0$ then the first equation yields: 1) $\sinh\xi = 0$, or; 2)

$$\cosh\xi\cos(2\eta) = \sin\eta \tag{149}$$

Substituting $\xi = 0$ in the second equation (148) yields

$$\cos\eta(1 + \sin\eta) = k, \tag{150}$$

which has exactly one positive and one negative root on $(-\frac{\pi}{2}, \frac{\pi}{2})$. The latter root is denoted $x(0)$, see Fig. 19

To analize the remaining roots of (147) with $z = 0$, we substitute

$$\cosh\xi = \frac{\sin\eta}{\cos 2\eta} \tag{151}$$

into the second equation (148) with $z = 0$. After some algebra, we obtain

$$\sin^3 2\eta + 2k\sin^2 2\eta - 2k = 0 \ . \tag{152}$$

Introducing $u = \sin 2\eta$, we can rewrite (152) as

$$m(u) = u^3 + 2ku^2 - 2k = 0 \ . \tag{153}$$

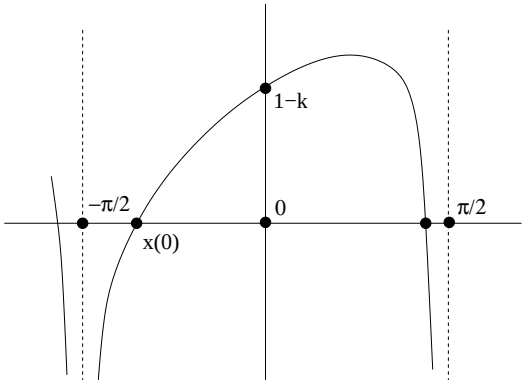

Figure 19: The graph of $\frac{1+\sin\eta}{\cos\eta} - \frac{k}{\cos^2\eta}$.

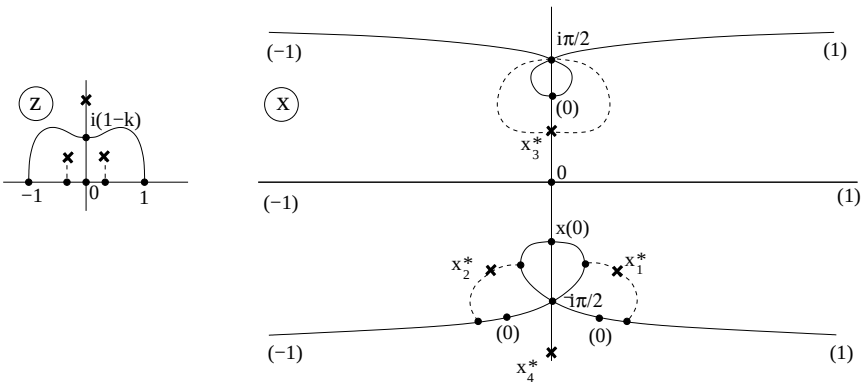

Figure 20: The image $\mathcal{C}$ and the domain $\mathcal{B}$ of the map $z = \alpha(x)$, where $\alpha(x)$ is defined by (139). Ramification points x_i^*, $i = 1, 2, 3, 4$ in the x-plane and the corresponding log points in $\mathcal{C}$ are marked by "crosses". Vertical cuts in $\mathcal{C}$ and their pre-images in $\mathcal{B}$ are shown by dashed lines. Round brackets in the x-plane are used to denote pre-images of points. The region $\mathcal{C}$ consists of the upper z-halfplane with three cuts. The upper boundary of $\mathcal{B}$ consists of two curves, connecting the pre-images of ± 1 with $\frac{i\pi}{2}$ (pre-images of $z > 1$ and $z < -1$ respectively), and the closed dashed curve (the pre-image of the cut from $\alpha(x_3^*)$ to $i\infty$). The lower boundary of $\mathcal{B}$ consists of two dashed curves that contain points x_1^*, x_2^* (pre-images of verical cuts in $\mathcal{E}^+$), the curve that connects them and passes through $x(0)$, and curves connecting the dashed curves with $\pm\infty$ (the latter three curves form a pre-image ob the interval $(-1, 1)$).

It is easy to see that $m(u)$ has a real root $u(k) \in [0,1)$. Let us show that $m(u)$ has only one real root. Indeed, $m'(u) = (3u+4k)u$. So, critical points of $m(u)$ are $u_1 = -\frac{4k}{3}$ and $u_2 = 0$. It is clear that u_1 is a local maximum, u_2 is a local minimum and $m(u_2) < 0$. Since $m(u_1) = \left(\frac{32}{27}k^2 - 2\right)k \leq 0$ for all $k \in [0,1]$, we conclude that $m(u)$ has a unique real root $u(k)$ and $u(k) \in [0,1)$.

Thus, we obtain $\sin 2\eta \in [0,1)$, which means $2\eta \in [0,\pi]$ or $2\eta[-2\pi,-\pi]$. That means $\eta \in [0,\frac{\pi}{2}]$ or $\eta \in [-\pi,-\frac{\pi}{2}]$. However, according to (151), we have a restriction

$$\frac{\sin\eta}{\cos 2\eta} \geq 1, \tag{154}$$

which imply that

$$\sin\eta < -\frac{1}{\sqrt{2}} \qquad \text{or} \qquad \frac{1}{2} \leq \sin\eta < \frac{1}{\sqrt{2}}\ . \tag{155}$$

Combining (155) with the above restrictions on η, we obtain

$$-\frac{3\pi}{4} < \eta < -\frac{\pi}{4} \qquad \text{or} \qquad \frac{\pi}{6} \leq \eta < \frac{\pi}{4}. \tag{156}$$

However, we will show that latter option is not possible. Indeed, implicitly differentiating (153), we obtain

$$\frac{du}{dk} = \frac{2(1-u^2)}{(3u+4k)u} > 0$$

for any $u \in (0,1)$. Thus, the root $u(k)$ is monotonically increasing. Substituting $u(k) = \sin 2\eta = \sin\frac{\pi}{3}$ into (153), we obtain the corresponding $k = \frac{3\sqrt{3}}{4} > 1$. Thus, for all $k \in [0,1]$, the corresponding $u(k) < \frac{\sqrt{3}}{2}$, so that (154) cannot be satisfies for the corresponding η.

Thus, we proved that for any $k \in [0,1]$ there exists a unique η and unique $\cosh\xi$, connected through (151), that satisfy (148). Moreover, such $\eta \in \left(-\frac{3\pi}{4},-\frac{\pi}{4}\right)$. Thus, we proved existence of the second pair of roots of $\alpha(x) = 0$ located in the strip $-\frac{3\pi}{4} < \Im x < -\frac{\pi}{4}$ and symmetrical with respect to the imaginary axis.

Obtained information allows us to sketch the domain $\mathcal{B}$ for the map (138), see Fig. 20. Calculation of $w(z)$ and of the jumps $\Delta f_0(z)$ over the branchcuts is not included into this paper.

References

[1] Bracewell, R., The Fourier Transform and its Applications, New York: McGraw-Hill, 1965.

[2] Bronski, J. C., Semiclassical eigenvalue distribution of the Zakharov-Shabat eigenvalue problem, *Phys. D* , 97 (1996), no. 4, 376-397.

[3] Cai, D., McLaughlin, D.W. and McLaughlin, K.T.R., The nonlinear Schrödinger equation as both a PDE and a dynamical system. *Handbook of dynamical systems*, Vol. 2, 599-675, North-Holland, Amsterdam, 2002.

[4] Ceniceros, H. and Tian, F.-R., A numerical Study of the semi-classical limit of the focusing nonlinear Schrödinger equation, *Phys. Lett. A*, 306 (2002), no. 1, 25-34.

[5] Dubrovin, B., Grava, T., and Klein, C., On Universality of Critical Behavior in the Focusing Nonlinear Schrdinger Equation, Elliptic Umbilic Catastrophe and the Tritronque Solution to the Painlev-I Equation, *Journal of Nonlinear Science*, 19 (2009) no. 1, 57 - 94.

[6] Deift, P., Kriecherbauer, T., McLaughlin, K. T.-R., Venakides, S. and Zhou, X., Uniform asymptotics for polynomials orthogonal with respect to varying exponential weights and applications to universality questions in random matrix theory. *Comm. Pure Appl. Math.* 52 (1999), no. 11, 1335-1425.

[7] Deift, P.and McLaughlin, K. T-R., A continuum limit of the Toda lattice. *Mem. Amer. Math. Soc.* 131 (1998), no. 624, 216pp.

[8] Deift, P., Venakides, S. and Zhou, X., New results in small dispersion KdV by an extension of the steepest descent method for Riemann-Hilbert problems. *Internat. Math. Res. Notices* 6 (1997), 286-299.

[9] Deift P.; Zhou, X. A steepest descent method for oscillatory Riemann - Hilbert problems. Asymptotics for the mKdV equation. *Ann. of Math.* 137 (1993), 295-370.

[10] Deift P. and Zhou, X., Asymptotics for the Painlevé II equation. *Comm. Pure and Appl. Math.* 48 (1995), 277-337.

[11] Forest, M.G. and Lee, J.E., Geometry and modulation theory for the periodic nonlinear Schrodinger equation, in: C. Dafermos, et. al. (Eds.), Oscillation Theory, Computation, and Methods of Compensated Compactness, Vol. 2, IMA, Springer, New York, 1986.

[12] Gakhov F.D., Boundary value problems, Addison-Wesley Publishing Co., Reading, Mass.-London, 1966

[13] Kamvissis, S., McLaughlin, K. T.-R. and Miller, P., Semiclassical Soliton Ensembles for the Focusing Nonlinear Schrödinger Equation, Annals of Mathematics Studies, v. 154, Princeton University Press, Princeton, 2003.

[14] Lyng, G. and Miller, P., The N-Soliton of the Focusing Nonlinear Schrödinger Equation for N Large, *Comm. Pure Appl. Math.*, 60 (2007), no. 7, 951-1026.

[15] Miller P. D. and Kamvissis, S., On the semiclassical limit of the focusing nonlinear Schrdinger equation. *Phys. Lett.* A 247 (1998), no. 1-2, 75-86.

[16] Miller P.D., Some remarks on a WKB method for the non self-adjoint Zakharov-Shabat eigenvalue problem with analytic potentials and fast phase, *Physica D* 152-153 (2001) 145-162.

[17] Shabat, A. B., One-dimensional perturbations of a differential operator and the inverse scattering problem. *Probelms in Mechanics and mathematical physics*, Nauka, Moscow 1976.

[18] Servat, E. and Tovbis, A., On the semiclassical limit of the eigenvalue problem for the focusing nonlinear Schrödinger equation: the WKB approach, Preprint (2005).

[19] Satsuma, J. and Yajima, N., *Suppl. Prog. Theor. Phys.* 5 (1974), 284.

[20] Tovbis, A. and Venakides, S., The eigenvalue problem for the focusing nonlinear Schrdinger equation: new solvable cases. *Phys. D* 146 (2000), no. 1-4, 150-164.

[21] Tovbis, A. and Venakides, S., Nonlinear steepest descent asymptotics for semiclassical limit of integrable systems: Continuation in the parameter space, arXiv:0902.1123 (2009).

[22] Tovbis, A., Venakides, S. and Zhou, X., On semiclassical (zero dispersion limit) solutions of the focusing Nonlinear Schrödinger Equation. *Comm. Pure Appl. Math.* 57, no. 7 (2004), 877-985.

[23] Tovbis, A., Venakides, S. and Zhou, X., On the long time limit of semiclassical (zero dispersion limit) solutions of the focusing Nonlinear Schrödinger Equation: Pure radiation case. *Comm. Pure Appl. Math.* 59, no. 10 (2006), 1379-1432.

[24] Tovbis, A., Venakides, S. and Zhou, X., Semiclassical focusing Nonlinear Schrödinger Equation I: Inverse scattering map and its evolution for radiative initial data *IMRN* (2007), accepted.

[25] Zakharov, V. E. and Shabat, A. B., Exact theory of two-dimensional self-focusing and one-dimensional self-modulation of waves in nonlinear media, *Soviet Physics JETP* 34 (1972), No 1, 62-69.

[26] Zhou, X. The L2-Sobolev space bijectivity of the scattering and inverse scattering transforms, *Comm. Pure Appl. Math.*, 51 (1998), 697-731.

[27] Zhou, X., Riemann-Hilbert problems and integrable systems, Preprint (2000).